Geophysics Open-File Report 42
Geoscience Department and
Geophysical Research Center
New Mexico Tech
Socorro, NM 87801
May, 1983

THE MAPPING OF SHALLOW MAGMA BODIES NEAR SOCORRO, NEW MEXICO, BY THE USE OF SEISMIC ATTENUATION

by

Jeffrey M. Roach

Submitted in partial fulfillment

of the requirement for

Geophysics 590

and the

Master's Degree Program

at

New Mexico Institute of

Mining and Technology

MAY, 1982

ABSTRACT

Data from a movable array of high-gain short-period seismographs were used to locate areas believed to contain magma in the central region of the Rio Grande rift near Socorro, New Mexico. Microearthquakes were recorded over a period of 316 recording days from May 1975 through January 1978. The locations of earthquakes and the ratio of the amplitudes of the P and SV phases on the seismograms were used in the study.

Corrections were made to the observed P to SV ratios to account for differences in dominant frequency of the P and SV phases, the angle of incidence of the incoming seismic waves, and differential seismic attenuation of the P and SV phases. Using known fault plane mechanisms, the expected theoretical ratio for all raypaths was computed. If observed ratios exceeded theoretical ratios by a factor of two the raypath was considered anomalous. Three-dimensional mapping of anomalous raypaths made it possible to identify specific volumes of crustal material believed to contain magma.

The study revealed three anomalous crustal regions located above the large (1700 km^2) mid-crustal magma body which lies at a depth of about 19 km. The proposed bodies are dike shaped and range in depth from 4.5 km to 10 km. The magma in these anomalous bodies is fairly widely

disseminated as suggested by the proportion of non-anomalous raypaths which pass through them.

TABLE OF CONTENTS

Introduction.....1

Physical Parameters for Socorro Area.....4

Data.....6

Location of Anomalous Crust.....19

Discussion.....25

Conclusions.....38

Acknowledgements.....39

References.....40

Appendix I.
Data used for the determination
of anomalous behavior.....43

Appendix II.
A listing of composite fault plane
solutions as deduced by Wieder (1981).....53

Appendix III.
Computer programs for plotting
raypaths in two dimensions.....54

Appendix IV.
Cross-sectional and areal
views of anomalous raypaths.....60

Appendix V.
Cross-sectional and areal
views of non-anomalous raypaths.....76

INTRODUCTION

Seismic waves which pass through crustal areas containing melt are characterized by greater attenuation of the shear wave than the compressional wave. By identifying and mapping raypaths which show this attenuation, it should be possible to locate crustal areas with magma. Using microearthquake data recorded by a movable array near Socorro, New Mexico, I have studied this type of attenuation to map regions in the upper crust of the Rio Grande rift where magma is believed to exist.

The area of study is located within the Rio Grande rift (figures 1 and 2), which is a north-south trending structure formed by an east-west tensional stress field. Geological evidence suggests that structural extension has been occurring for the past 30 million years (Chapin and Seager, 1975). In depth studies and interpretations have been compiled on the geophysical characteristics of the Rio Grande rift. These may be found in Chapin (1971), Chapin and Seager (1975), Sanford et al. (1977), Cordell (1978), and Rio Grande Rift: Tectonics and Magmatism edited by Riecker (1979).

The microearthquakes in the area near Socorro are centered over a 1700 km^2 sill-like magma body which is located at a depth of 19.2 ($\pm$ 0.6)km. The mid-crustal magma body was first identified through an analysis of strong SxS

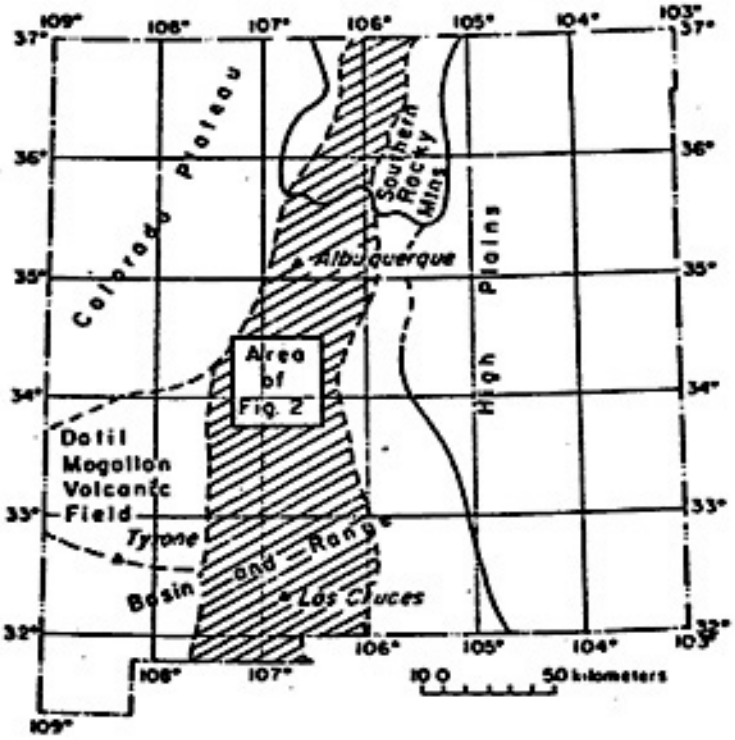

Figure 1. Physiographic provinces and the Rio Grande rift in New Mexico (after Chapin, 1971). Also shown is the approximate area contained in Figure 2.

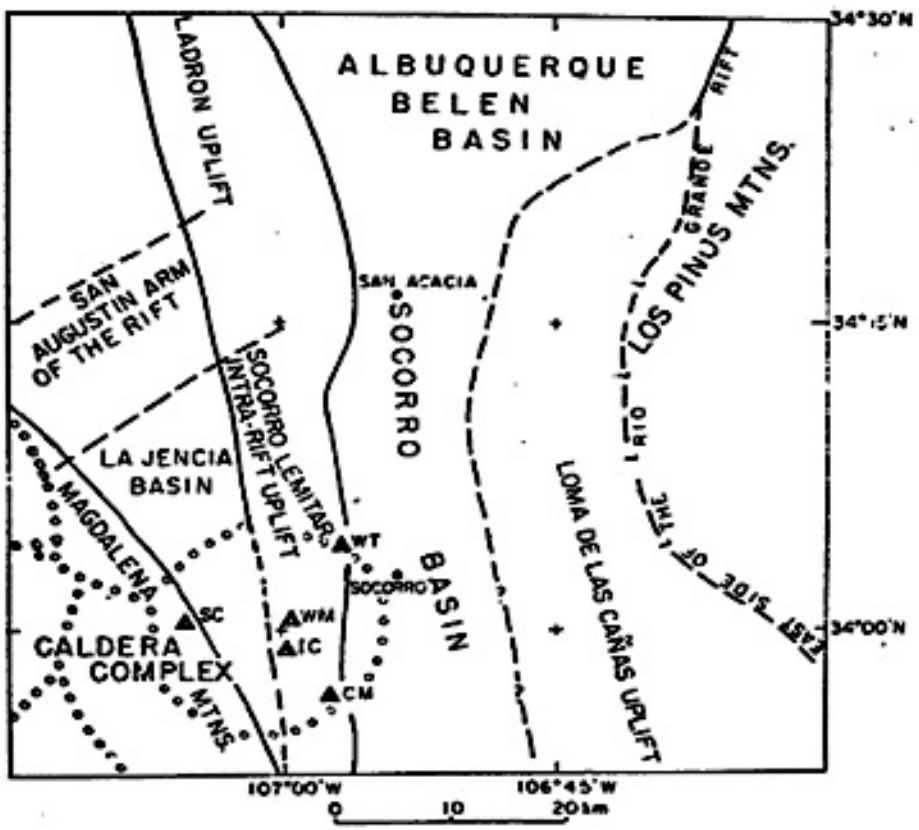

Figure 2. Major physiographic features near Socorro and locations of seismic stations used.

reflections from microearthquakes (Sanford and Long, 1965; Sanford et al., 1973; Sanford et al., 1977; and Rinehart et al., 1979). At a later time COCORP profiling showed a strong P wave reflection from the same depth (Brown et al., 1979; Brown et al., 1980).

In other studies using microearthquake data, evidence for shallower magma bodies was found. Screening of S waves from microearthquakes (Shuleski, 1976; Johnston, 1978), distinctly high Poisson ratios (Caravella, 1976; Fender, 1978; Frishman, 1979), and a low compressional wave velocity zone in the upper crust (Ward, 1980) provide most of the evidence for shallow magma bodies. Reviews of the geophysical studies on shallow magma bodies may be found in Chapin et al. (1978), Guidebook to the Rio Grande Rift in New Mexico and Colorado edited by Hawley (1978), and Sanford and Schlue (1980).

PHYSICAL PARAMETERS FOR SOCORRO AREA

Before an accurate study could be undertaken, physical parameters had to be prescribed. The first parameter determined was the surface P wave velocity, a parameter required for the calculation of the corrected angle of incidence. Of the five recording stations used for this study, four are in basically the same geologic setting. Stations CM, IC, SC, and WM are located on thick sections of volcanic rock within the Socorro cauldron. These stations have a similar geologic setting to station CT where measurements of the angles of incidence for microearthquakes and explosions were conducted several years ago (Sanford, personal communication, 1982). Knowing the average angle of incidence (22.1°) and the crustal P wave velocity (5.80 km/s), the velocity of the surface rock at station CT was found to be $Vp = Vmax(\sin io) = 2.20$ km/s. This velocity was used for near surface rock at stations CM, IC, SC, and WM. The remaining station in the study, WT, is located on highly fractured Precambrian rock. A seismic profile across this rock indicated a velocity of 2.65 km/s.

A crustal S wave velocity was calculated by the use of a Poisson ratio of 0.25 (Caravella, 1976; Fender, 1978). The resulting velocity was 3.35 km/s. Note that the value I have used for Vp is slightly less than that observed by Ward (1980) and the value of Vs is slightly smaller than that obtained by Rinehart (1979). The minimum quality factor Q

for the P wave in the Rio Grande rift has been determined by Brocher (1981) to be 625. By using the results of Winkler and Nur (1982) that the average Qp/Qs is close to 1.0, I have made all calculations using Qp = Qs = 625.

DATA

The microearthquakes used for this study were obtained from a movable array of seismic recording instruments. The array was set up near Socorro, New Mexico at a number of seismic recording sites which have known spacial coordinates. Locations for these events were obtained by using HYPO71, an earthquake location program developed by Lee and Lahr (1975). Details of the procedure and parameters used for these solutions are described by Wieder (1981).

Measurements were made of the P and S phase amplitudes (one-half peak to peak) of each event. Only events with P amplitudes greater than 2mm were used because amplitudes for weaker events were considered uncertain. A data set of amplitudes was compiled and is listed in Appendix I.

The present stress field near Socorro has been deduced by Wieder (1981) through the construction of composite fault-plane solutions for twelve distinct geographic areas. The resulting solutions from this work are listed in Appendix II. The solutions for seven of the geographic areas are well constrained and high confidence is placed on them and are so marked in the listing of these solutions. The other five do not carry as high a confidence. Details of the solution quality for each area may be found in Wieder (1981). A pictorial view of Wieders results is found in

figure 3.

Theoretically, by knowing the fault-plane solution for a specific area, it is possible to calculate the expected amplitude ratio along a prescribed raypath from the focus given the azimuth and angle of emergence of the raypath. With this information, and using a program written for the Hewlett-Packard HP97 calculator by Bruce Julian (Allan Sanford, personal communication, 1982), these ratios were computed. Given below is a sample calculation of the theoretical amplitude ratio for an event on 8/8/75 from area 5 which was recorded at station WT.

****

PLUNGE OF a	-44.00
AZIMUTH OF a	263.00
PLUNGE OF n	42.00
AZIMUTH OF n	292.00
DIP OF RAYPATH	-75.00
AZIMUTH OF RAYPATH	269.00
P AMPLITUDE	-0.80
SV AMPLITUDE	0.47
SH AMPLITUDE	-0.28
S AMPLITUDE	0.55

$$\text{RATIO} = \frac{|P|}{5.2|SV|} = \frac{|-0.80|}{5.2|0.47|} = 0.327$$

* Note, SV is multiplied by 5.2 since the amplitudes for the S as well as P are normalized to 1.0.

****

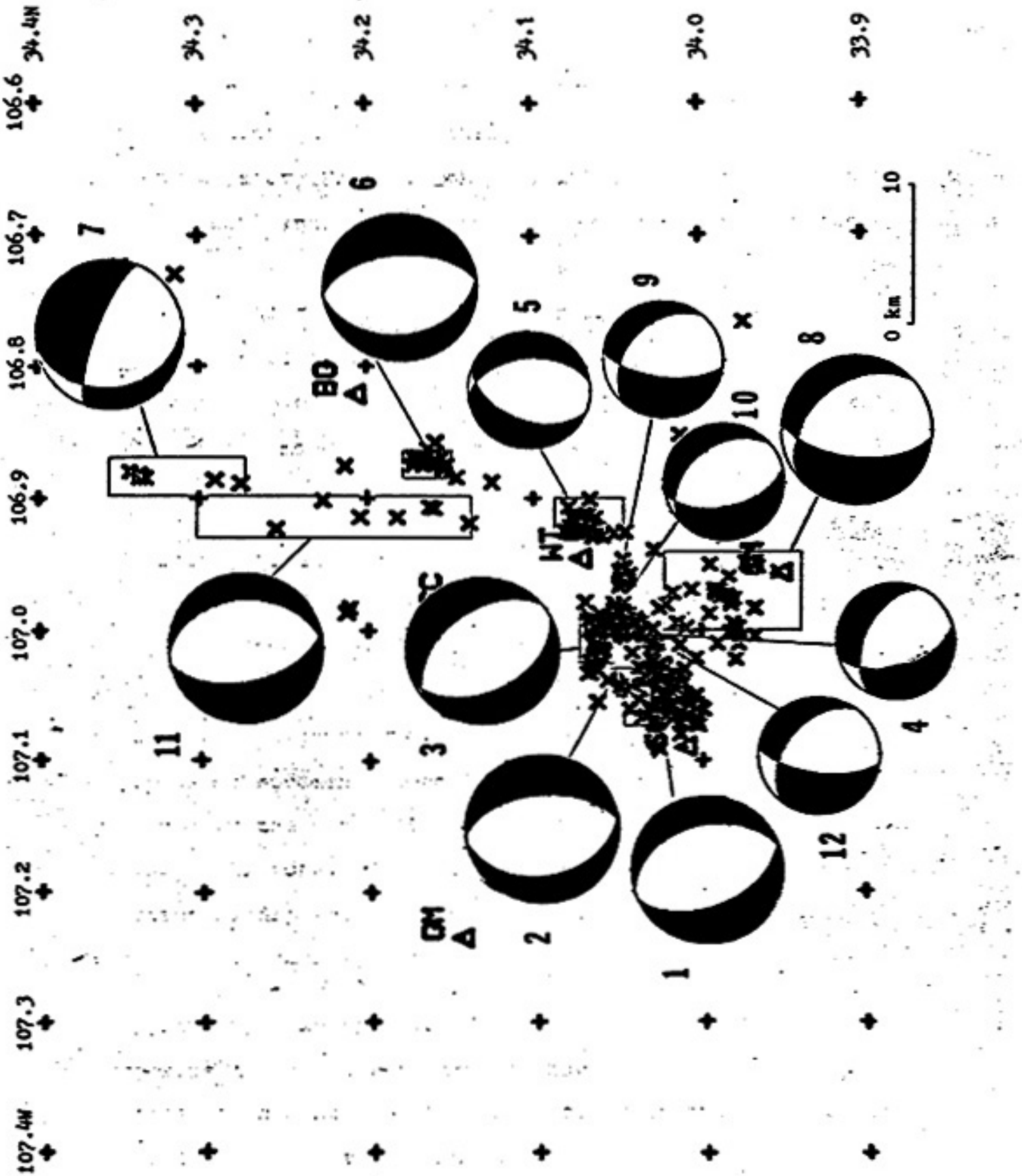

Figure 3. Composite fault-plane solutions for 12 geographic areas as deduced by Wieder. The well constrained solutions are designated by large circles and the others, which are based on P and T axes of the well constrained solutions, are denoted by small circles. The shaded areas represent regions of compressions and the white areas are regions of dilatations.

The measured amplitude ratios from the seismograms require correction before they can be compared with the theoretical values. The three corrections applied account for differences in the dominant frequency of the P and S waves, the angle of incidence of the incoming seismic wave at the recording station, and differential seismic attenuation of P and S waves. The first correction was made by multiplying the measured amplitude ratios by the ratio of the S to P dominant frequencies. Johnston (1978) determined that the dominant S frequency was 12.3 hz and the dominant P frequency was 19.7 hz.

A correction on the angle of incidence was made because seismic waves tend to refract to smaller angles as they approach a recording station through a low velocity layer. From Snell's law, $i_1 = \sin^{-1}[(V_1/V_2)\sin i_2]$, one can see from figure 4 that $i_2 \approx i_3$ where i_3 is the angle of incidence calculated from HYPO71. Differences between i_2 and i_3 are greatest for shallow depths of focus and small epicentral distances, for example, $i_2 - i_3$ is 6 degrees when the depth of focus is 6 km and the epicentral distance is 1.9 km. Inasmuch as the depth of focus is usually greater than 6 km and the epicentral distance greater than 1.9 km, the difference is less for nearly all cases in this study, (Sanford, personal communication, 1982). Once the corrected angle of incidence was calculated, the measured vertical component amplitude ratios were multiplied by the tangent of this angle to obtain the ratio of total amplitudes.

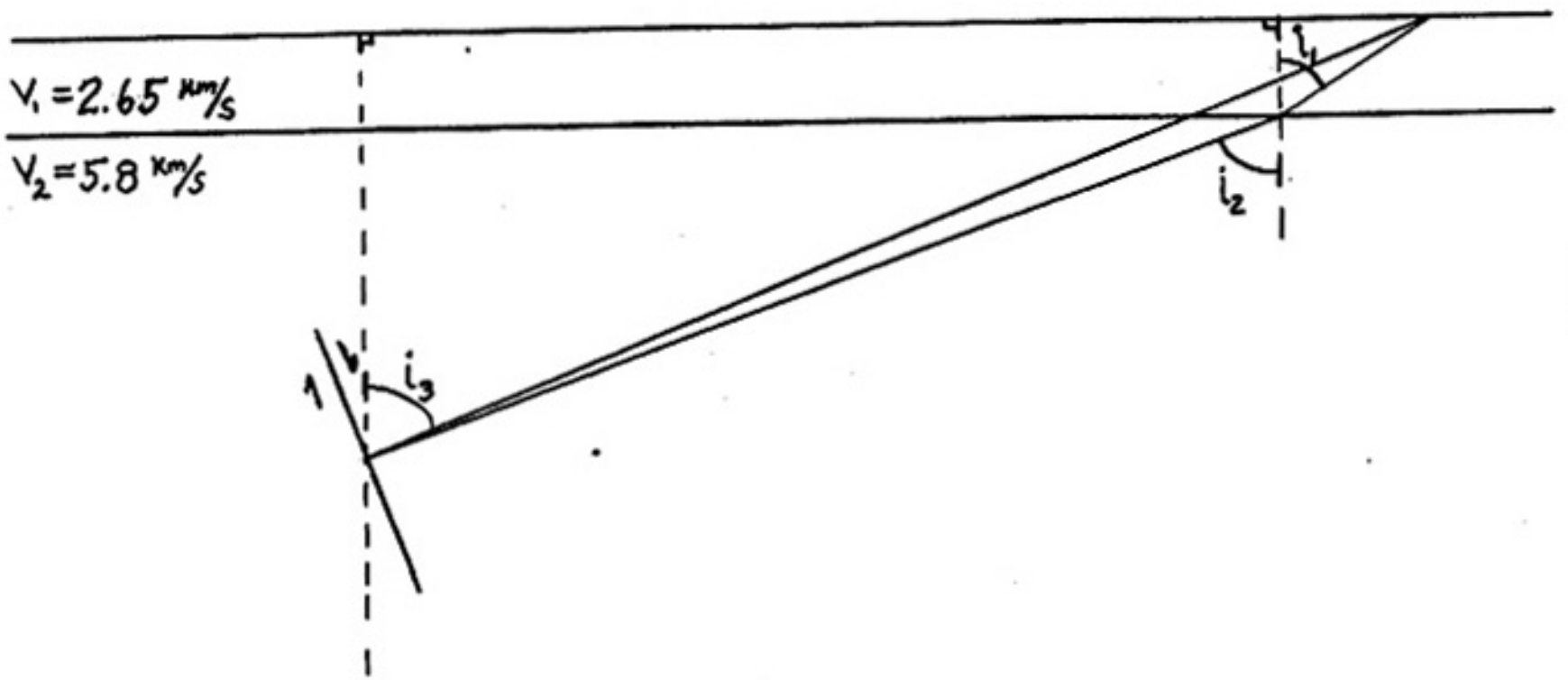

Figure 4. A two layer model of the upper crust which shows that $i_2 \approx i_3$. This information was used in obtaining a correction to the angle of incidence for the observed P to SV ratios.

Finally, a correction for the differential seismic attenuation was made. The measured amplitude ratios were multiplied by the term:

$$e^{\frac{r\pi f}{Q}\left[\frac{1}{Vp} - \frac{1}{Vs}\right]}$$

where Q, the quality factor, was assumed to be the same for P and S waves. This may not actually be the case but sample calculations indicated that very small differences in the final corrected ratios resulted when reasonable differences in these values were used. The term "f" is the average dominant frequency of the P and S waves. The term "r" is the slant distance from the hypocenter to the recording station and is calculated by simple geometry.

The final equation for the observed amplitude ratios is:

$$\frac{Ap}{Asv} = \frac{Wp}{Wsv} \quad \text{Tan ic}\left(\frac{f_s}{f_p}\right) \exp\left[\frac{r\pi f}{Q}\left(\frac{1}{Vp} - \frac{1}{Vs}\right)\right] \qquad (1)$$

Given below is a sample calculation for the event on 8/8/75 in area 5 which was recorded at station WT.

****

AMPLITUDE OF P PHASE: 9.50mm = Wp
AMPLITUDE OF S PHASE: 2.50mm = Wsv

From HYPO71: i = 14.4°

ic = corrected angle of incidence

$$ic = \sin^{-1}\left(\frac{V1}{V2}\sin i\right) = \sin^{-1}\left(\frac{2.65}{5.80}\sin 14.4^{\circ}\right) = 6.54^{\circ}$$

r = slant distance from hypocenter to station

$r = [(\text{epicentral dist.})^2 + (\text{depth})^2]^{1/2}$

$r = [(2.20\text{km})^2 + (8.54\text{km})^2]^{1/2} = 8.82$ km

From equation (1) in the text and using the physical model parameters discussed earlier we obtain:

$$\frac{Ap}{Asv} = \frac{9.50}{2.50}\left[\text{Tan } 6.54\right](0.62)\exp\left[\frac{8.82\,\pi\,16}{625}\left(\frac{1}{5.80} - \frac{1}{3.35}\right)\right] = 0.257$$

****

For each station in the study, a graph was constructed of the observed ratios versus the theoretical ratios (figures 5a through 5e). On these graphs, different symbols are used to indicate the area from which the data originates.

Figures 5a-5e. Graphs of observed vs. theoretical ratios for the events whose P phase vertical amplitude was greater than 2mm. Note that different symbols have been used for events from different geographic areas.

Area	Symbol	Area	Symbol
1	□	7	▽
2	+	8	△
3	×	9	◁
4	◇	10	▷
5	⊠	11	▷
6	⊕	12	▷

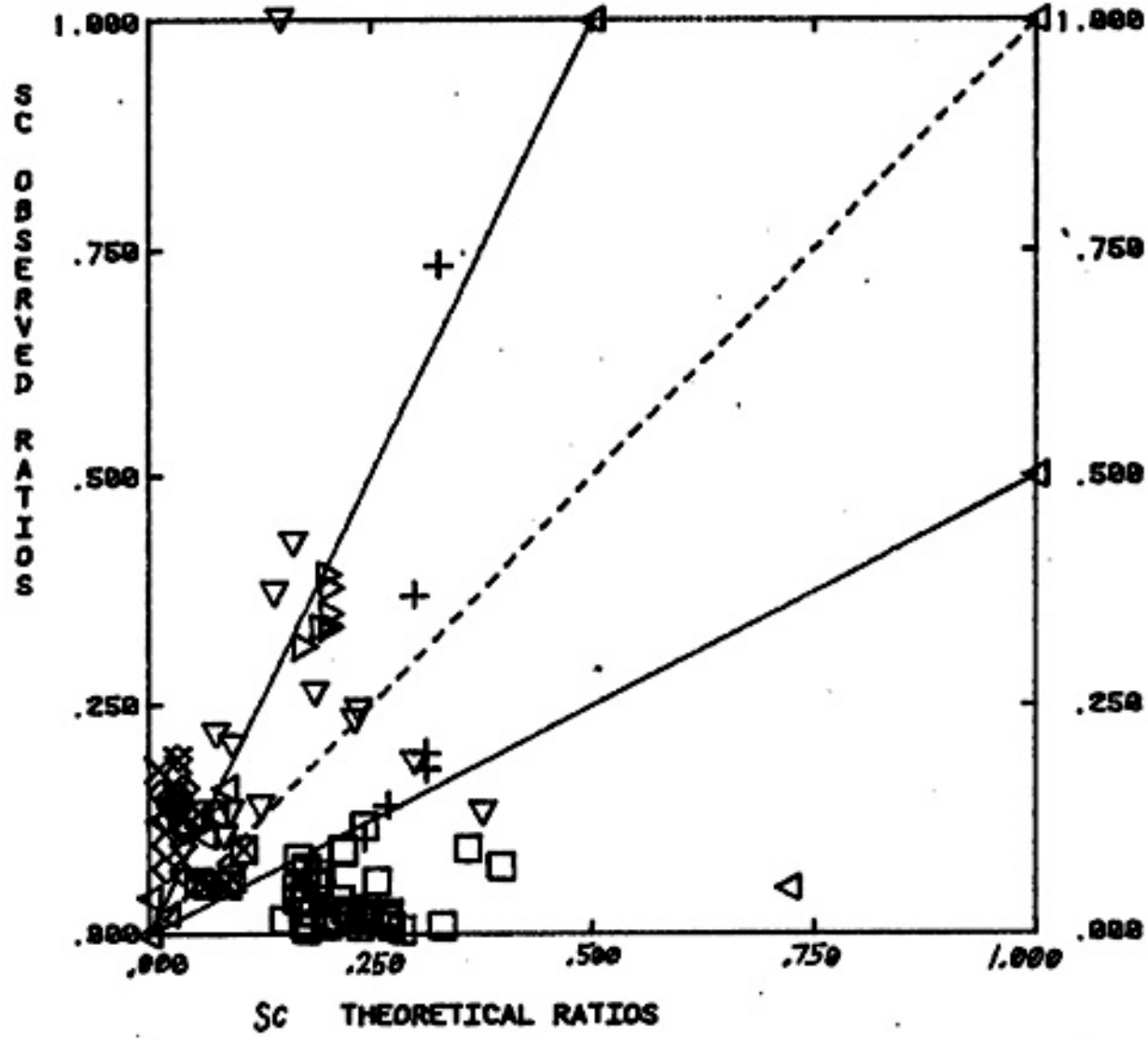
1.000
.750
.500
.250
.000
SC OBSERVED RATIOS
.000
.250
.500
.750
1.000
SC THEORETICAL RATIOS

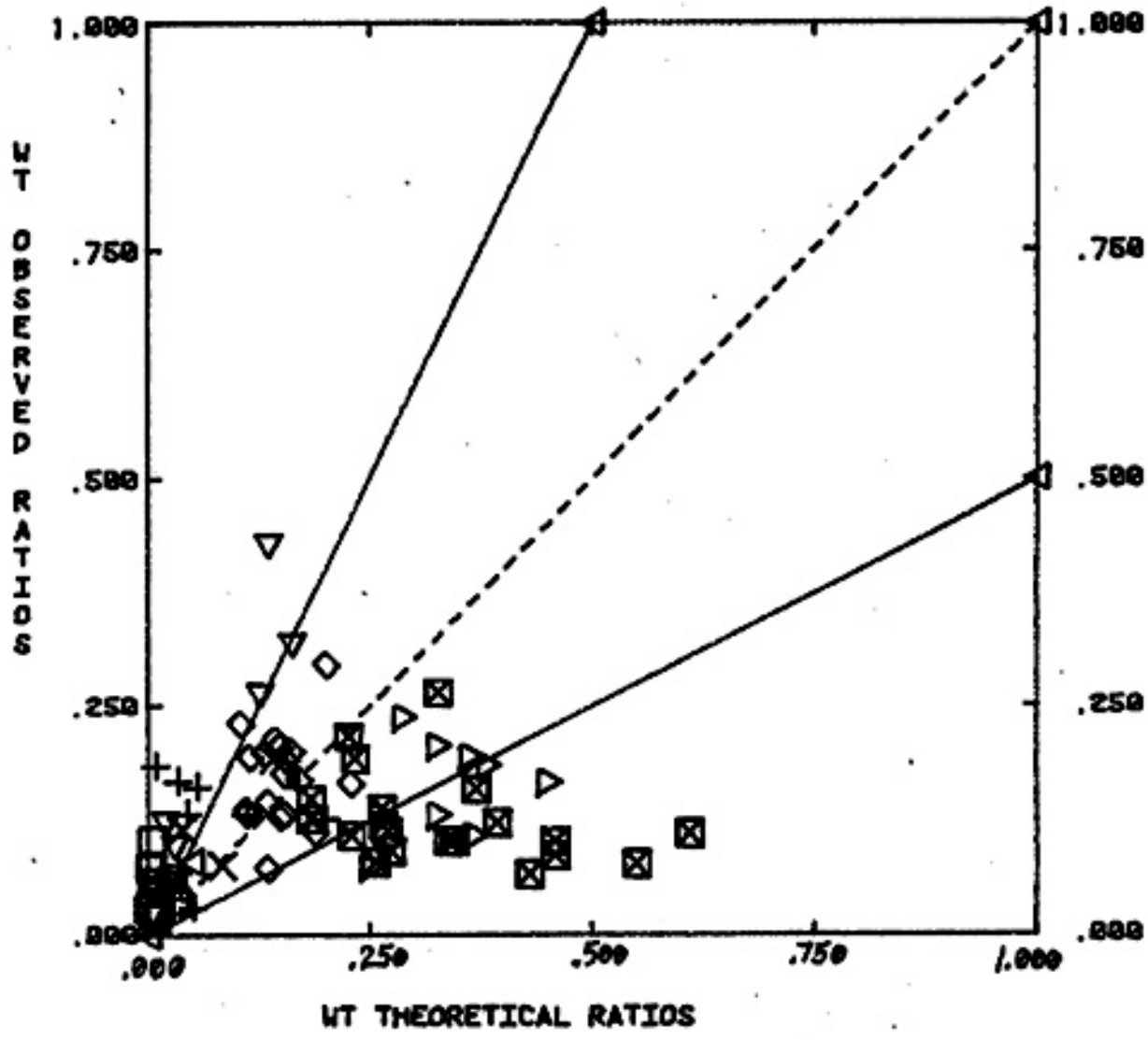
1.000
.750
.500
.250
.000
WT OBSERVED RATIOS
.000
.250
.500
.750
1.000
WT THEORETICAL RATIOS

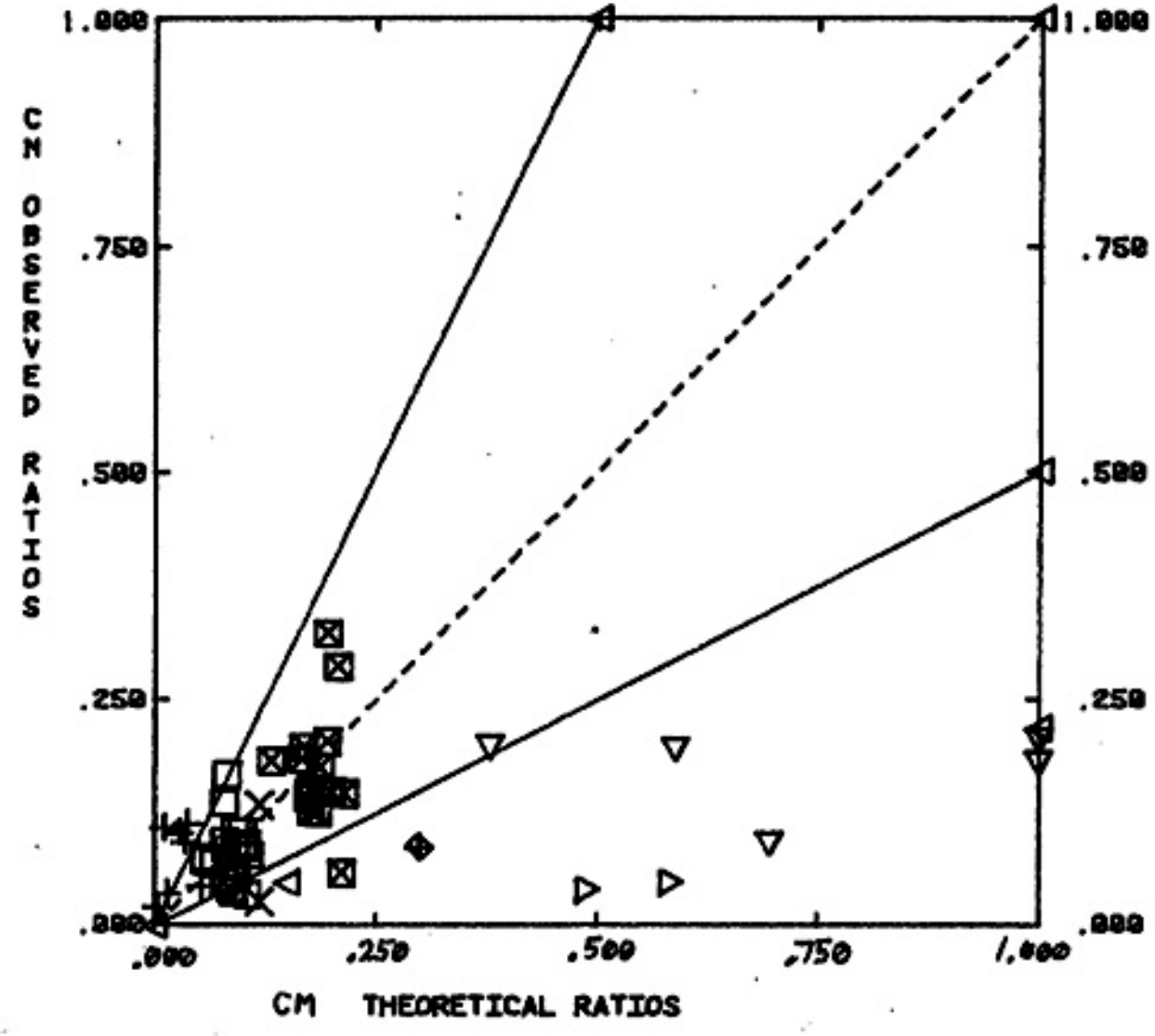
1.000
.750
.500
.250
.000
CN OBSERVED RATIOS
.000
.250
.500
.750
1.000
CM THEORETICAL RATIOS

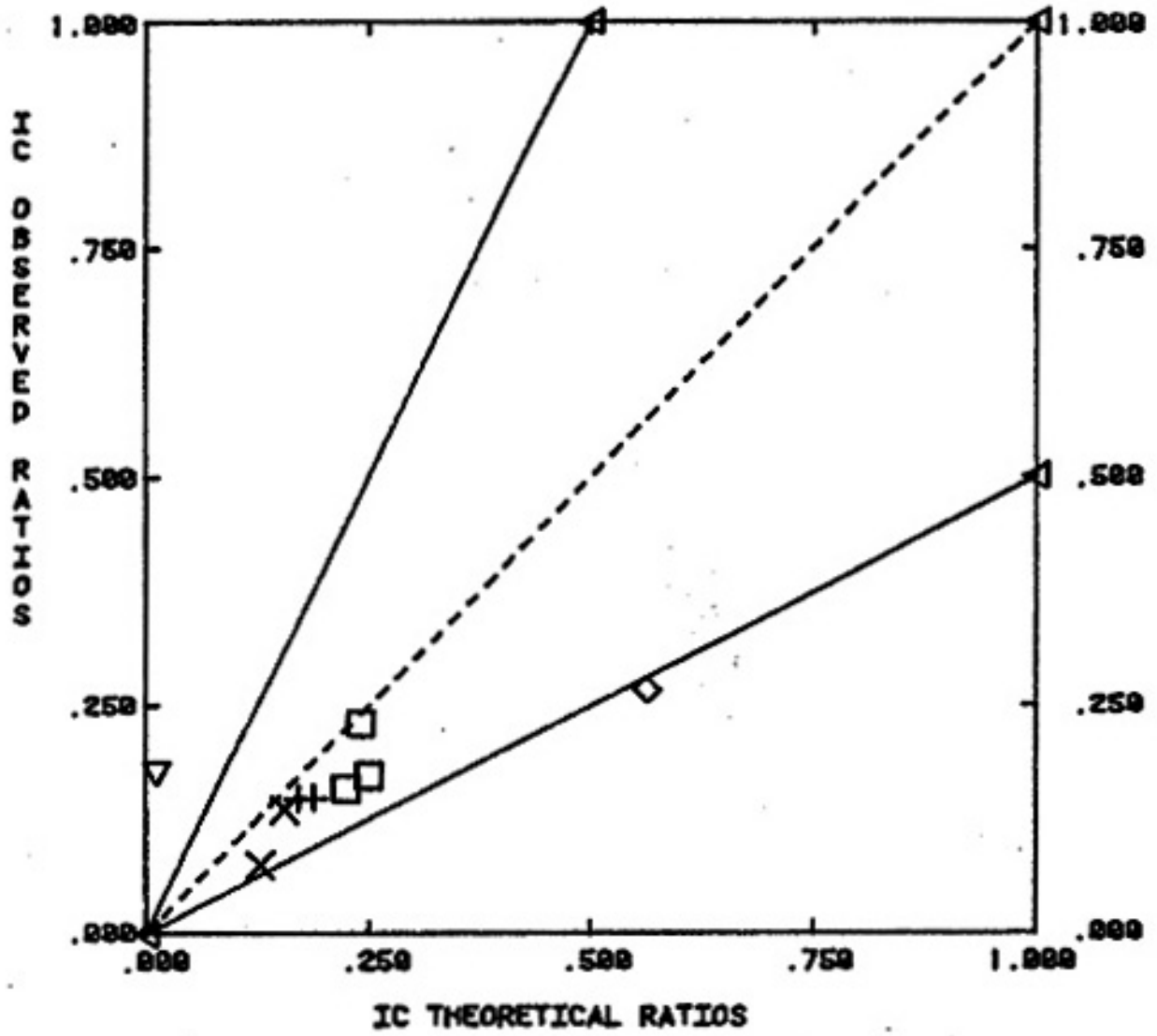
1.000
.750
.500
.250
.000
IC OBSERVED RATIOS
.000
.250
.500
.750
1.000
IC THEORETICAL RATIOS

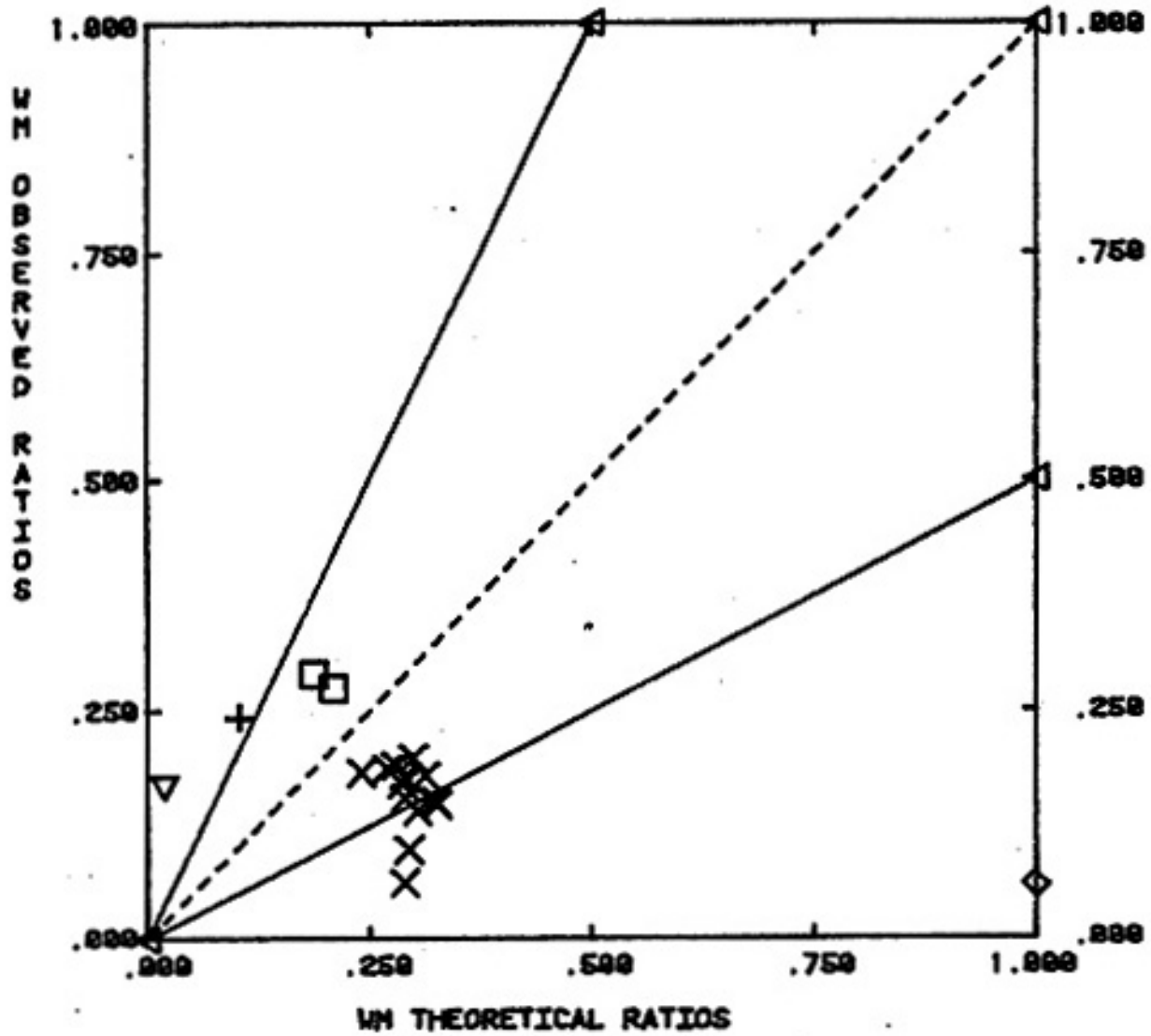
1.000
.750
.500
.250
.000
.000
.250
.500
.750
1.000
WM OBSERVED RATIOS
WM THEORETICAL RATIOS

LOCATION OF ANOMALOUS CRUST

As expected the diagrams of observed versus theoretical ratios show considerable scatter about a 45 degree line. For this study, it was arbitrarilly assumed that points falling below a line of slope 2.0 and above a line of slope 0.5 were normal.

Raypaths above the line with a slope of 2.0 were considered truly anomalous and are listed in Appendix I. In this region, one might also expect raypaths which leave the focal region on, or very close, to the P nodal plane. The theoretical ratios for these raypaths are very small while multi-pathing can cause the observed ratios to be quite large.

From the graphs of observed versus theoretical ratios, an estimate has been made of the actual number of events which travel on, or near, the P nodal plane. I have expanded the region of the plot near the lower limit and plotted ratios from all stations whose points fall above the line with a slope of 0.5. There is a lower limit of 0.019 for the observed ratios which indicates that because of multi-pathing we will never actually observe a ratio below this limit. I have made the assumption that all points falling below twice this value are for raypaths which have ratios expected near a P nodal plane. We now adjust the line distinguishing anomalous points from non-anomalous as

indicated by the curved dashed line in figure 6. This results in six data points being taken from the anomalous region (10.2% of the total anomalous paths). These six raypaths were retained in the analysis.

Data points below the lower limit, a slope of 0.5, can be explained by the fact that raypaths with hypocenters very near the recording station have small angles of incidence. Equation (1) indicates that a slight error in the angle when it is small leads to a very large error in the ratio. This can lead to very small observed ratios with respect to theoretical ratios. Sample calculations indicated that reasonable corrections for estimated errors in the angle i never moved these data points above the line of slope 2.0 and into the anomalous region. For this reason it was decided that no correction would be made for these raypaths because they would not be used in the study.

A listing of the anomalous raypaths may be found in Appendix I. The method for locating anomalous crust from the anomalous raypaths involved projections of the raypaths to each station on E-W, N-S cross-sections and on a horizontal plane. Programs were written which automatically drew the raypaths from the hypocenters to the stations for each projection. These programs are found in Appendix III. The results of these plotting routines are in Appendix IV.

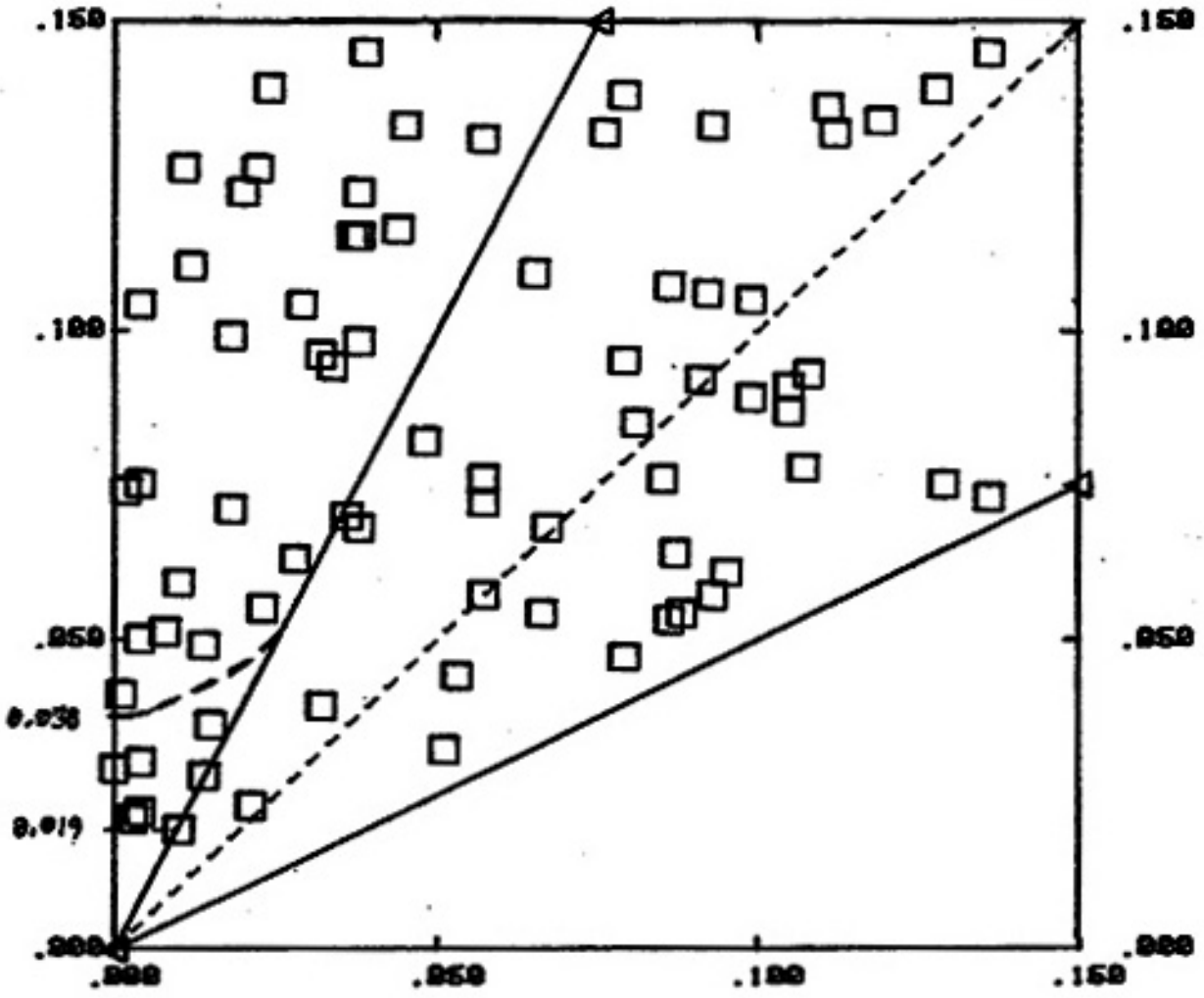

Figure 6. A graph of observed vs. theoretical ratios for all events whose P phase vertical amplitude was greater than 2mm and whose data point falls above the line of slope 0.5. A curved dashed line has been drawn to show the cutoff of events which are believed to travel on, or near, the P nodal plane.

Once the two dimensional plots were compiled, the process of locating anomalous crustal regions began. For this study, two assumptions were made. First, intersections of two of more anomalous raypaths were to be looked at as an indication of highest probability for anomalous crust.. Second, the positioning of the anomalous bodies would be centered, as much as possible, between the stations recording the anomalous raypaths in order to maximize the depth of the proposed anomalous regions.

The locating of the anomalous crust began by first overlaying the areal views and finding the regions with highest density of intersections. These were believed to give the areal extent of the anomalous regions. The resulting anomalous areas are given in figure 7.

Identification was then made of the raypaths passing through these regions so they could be distinguished in the other two projections. One proposed anomalous region was studied at a time. By using the method of overlaying projections, the vertical limits of the anomalous crustal regions were determined. Before the final configurations of the anomalous crust were determined, modifications in shape were made to account for the non-anomalous raypath data.

A majority of the raypaths in the study, 78.1 percent, are not anomalous. If these raypaths repeatedly pass through the abnormal crust defined by the anomalous raypaths, the method employed in this study for locating

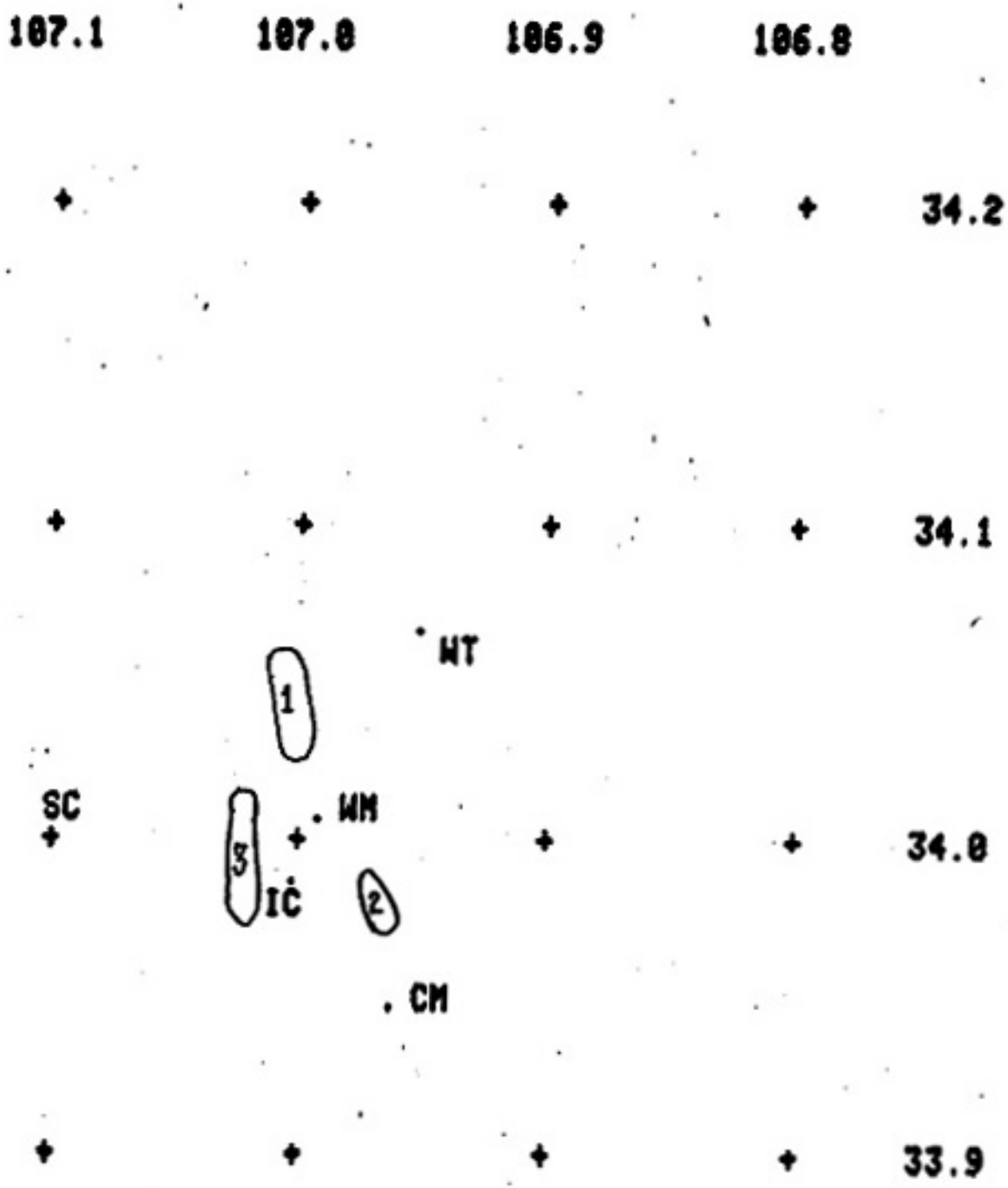

Figure 7. Areal views of the proposed anomalous crustal regions.

magma bodies would not be valid. The method used to study the distribution of non-anomalous raypaths was exactly the same as used for the anomalous raypaths. Data falling within the lines with slopes of 2.0 and 0.5 on figures 5a through 5e were used. A listing of all non-anomalous raypaths may be found in Appendix V.

DISCUSSION

In looking at the non-anomalous raypaths it was found that many passed through the crustal volumes defined by the anomalous raypaths. To be specific, 54 percent of the raypaths passing through body 1 were non-anomalous, 20 percent through body 2, and 55 percent through body 3. This suggests that the magma in these bodies is fairly widely disseminated. Minor changes to the shape of the bodies could be made to exclude a few of the non-anomalous raypaths but in general the non-anomalous raypaths passed through regions of the proposed bodies which were well defined by the anomalous paths. The resulting final model for the proposed anomalous crustal regions may be found in figures 7 and 8a through 8f. Finally it should be noted that, if the raypaths whose points on the graph fall between lines of slope 1.0 and 2.0 are excluded from the non-anomalous data set the percentage of non-anomalous paths penetrating the bodies becomes 26 percent for body 1, 20 percent for body 2, and 24 percent for body 3.

In general the crustal volumes defined by the anomalous raypaths are dike shaped and trend in the north-south direction. With the stress field as it is in the Rio Grande rift, and if intrusive bodies do exist, dikes would be the anticipated form. The depth to the magma in the anomalous crustal volumes ranges from about 4.5 km to 10.0 km .

Figures 8a-8f. Cross-sectional views of the three proposed anomalous crustal regions.

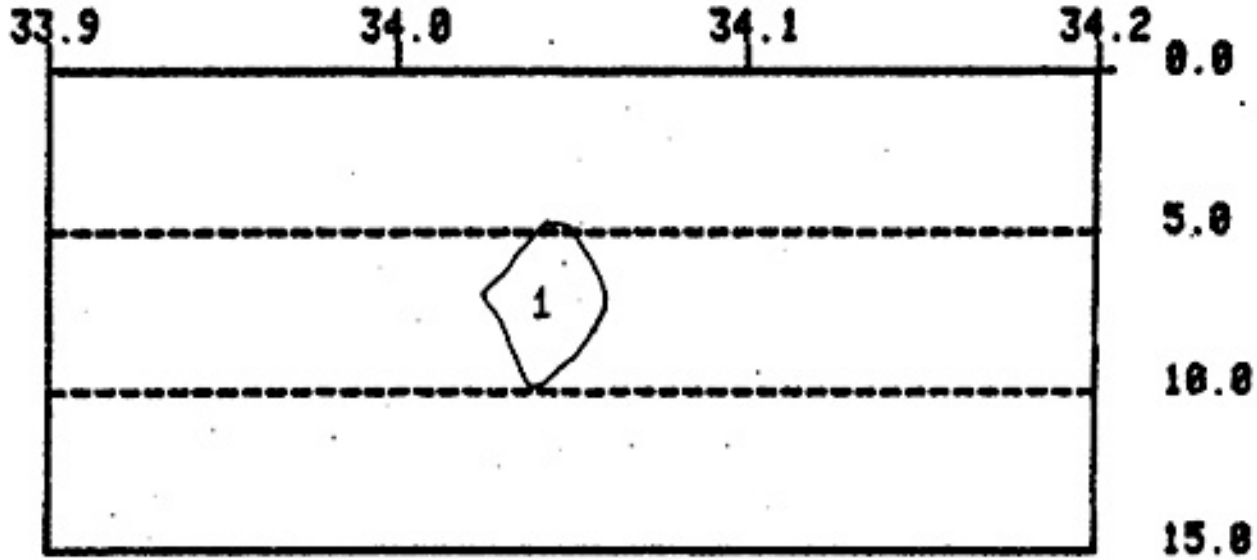
33.9
34.0
34.1
34.2
0.0
5.0
10.0
15.0
1

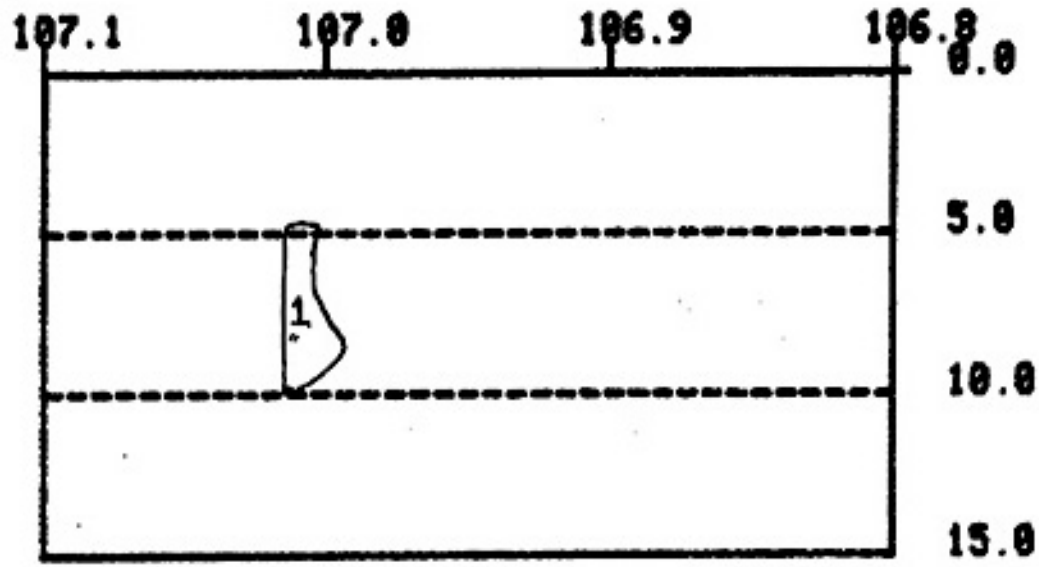
107.1
107.0
106.9
106.8
0.0
5.0
10.0
15.0
1

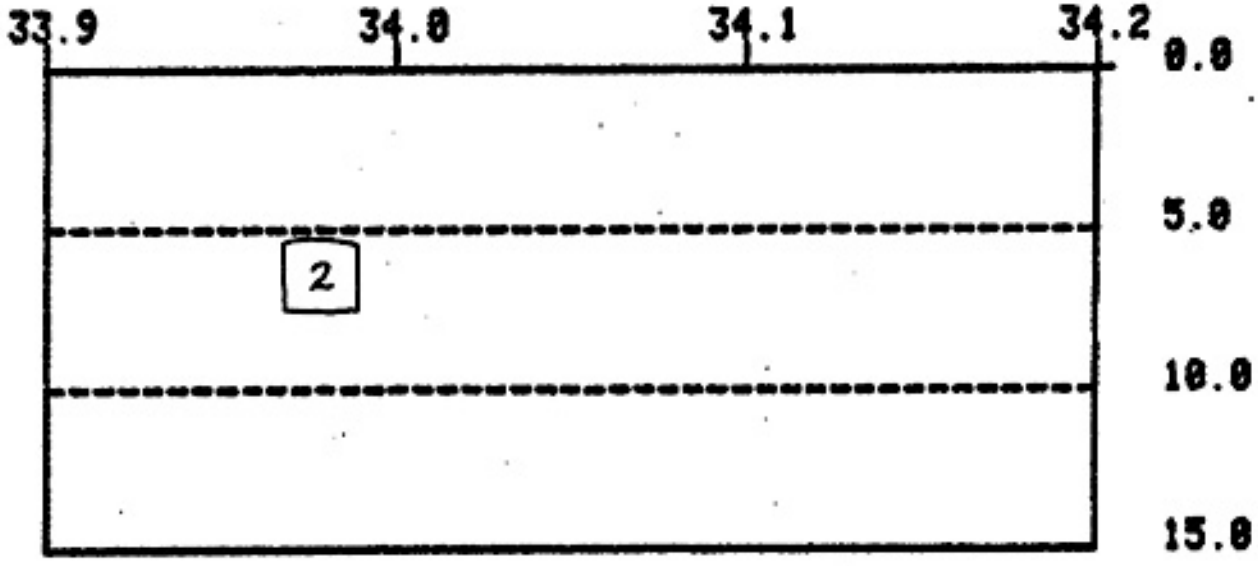
33.9
34.0
34.1
34.2
0.0
5.0
10.0
15.0
2

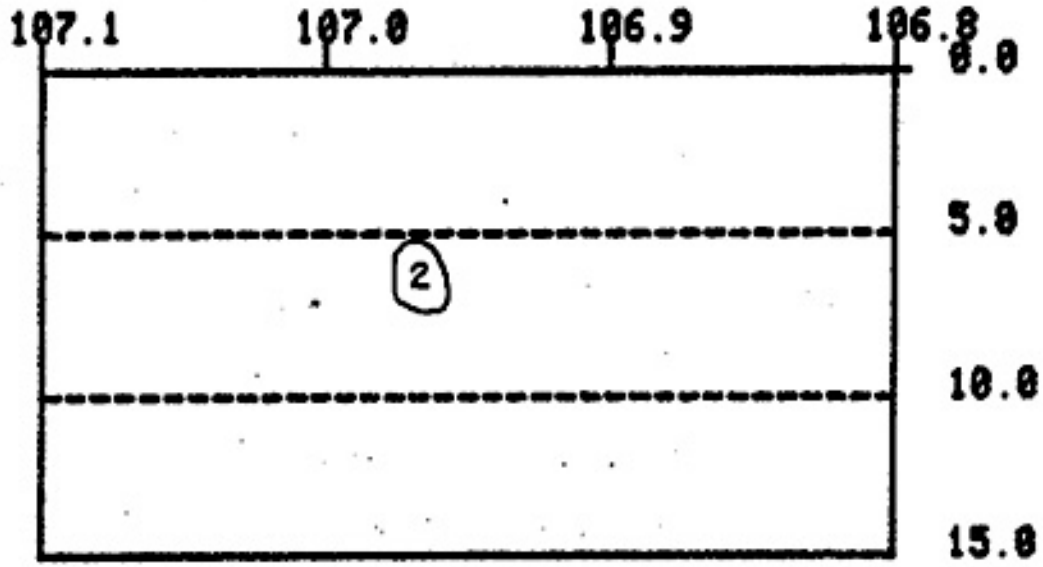
107.1
107.0
106.9
106.8
0.0
5.0
10.0
15.0
2

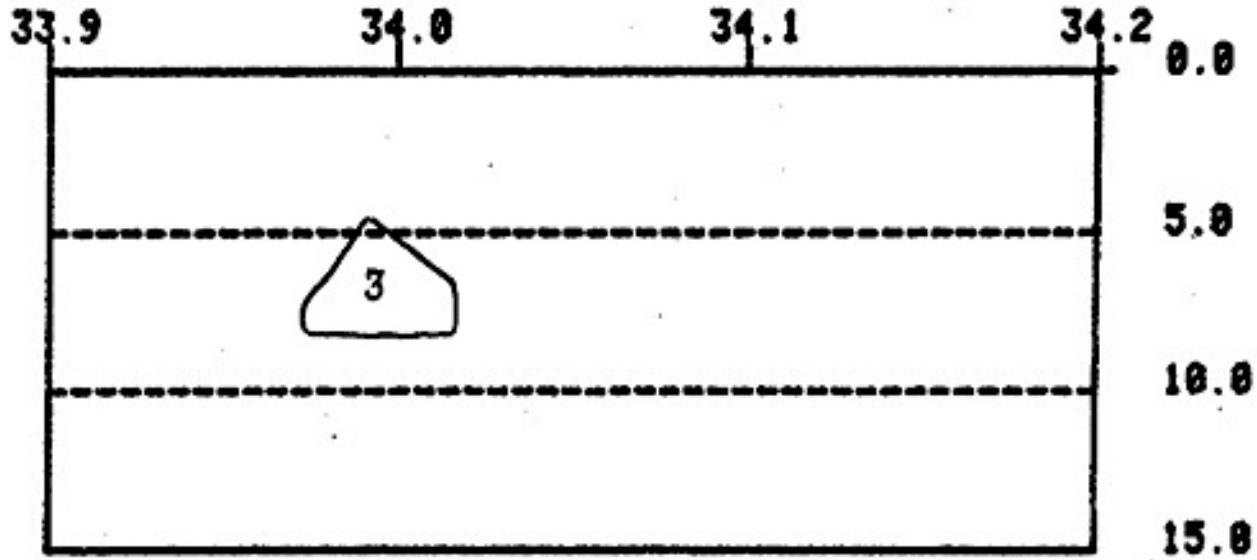
33.9
34.0
34.1
34.2
0.0
5.0
10.0
15.0
3

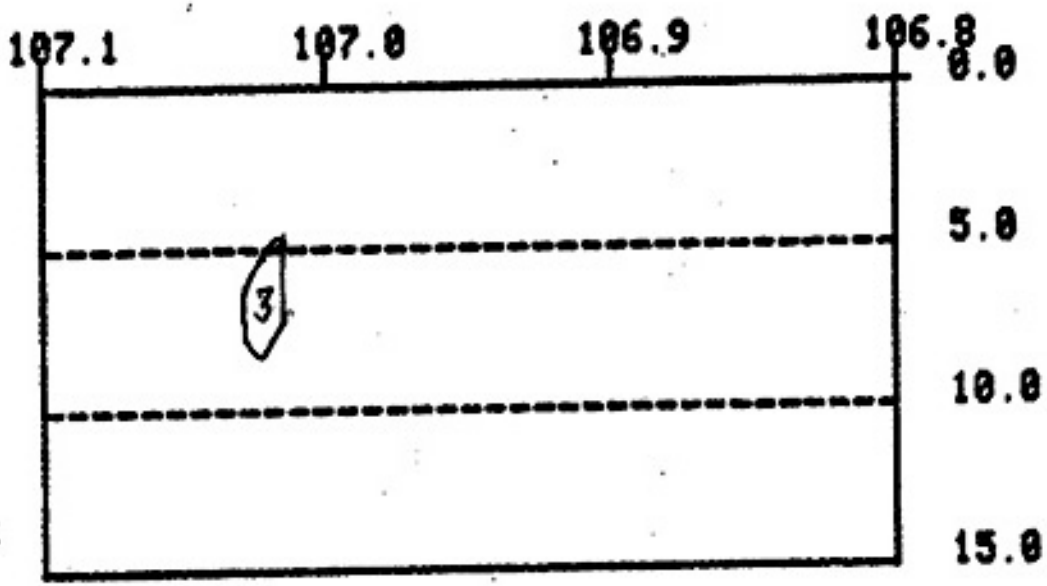
107.1
107.0
106.9
106.8
0.0
5.0
10.0
15.0
3

Previous work on the identification of shallow magma bodies in this area was completed by Johnston (1978), Ward (1980), and Shuleski (1976). The areal distributions of anomalous crust from these studies and my study are shown in figures 7,9,10, and 11. A comparison of my study with Johnston's shows that his area 5 has a position fairly close to area 2 in figure 7. If you look at area 1 and the northern portion of area 3 from my study you obtain an angular spread from stations SC, WM, and WT large enough to take into account Johnstons' proposed bodies 1, 3, and 4. The data are insufficient in this study to predict bodies corresponding to his areas 2, 6, 7 and 8.

Ward (1980) found that the crustal block below a depth of 4 km from 107.0° to 107.1° longitude and 34.0° to 34.1° latitude had an unusually low compressional wave velocity. This region does contain anomalous areas from my work. The northern portion of area 3 and all of area 1 from this study fall in his proposed anomalous region. Ward (1980) did not find a low velocity zone in block 106.9° to 107.0° longitude and 33.9° to 34.0° latitude where my study shows a small volume of anomalous crust (area 2).

In comparing the results of this study (figure 7) with that of Shuleski and Sanford (figure 11), one observes a closer agreement. If you consider my areas 1 and 3 as corresponding to their body 1 a fairly close correlation is found. Data in my work are inadequate to define a body in

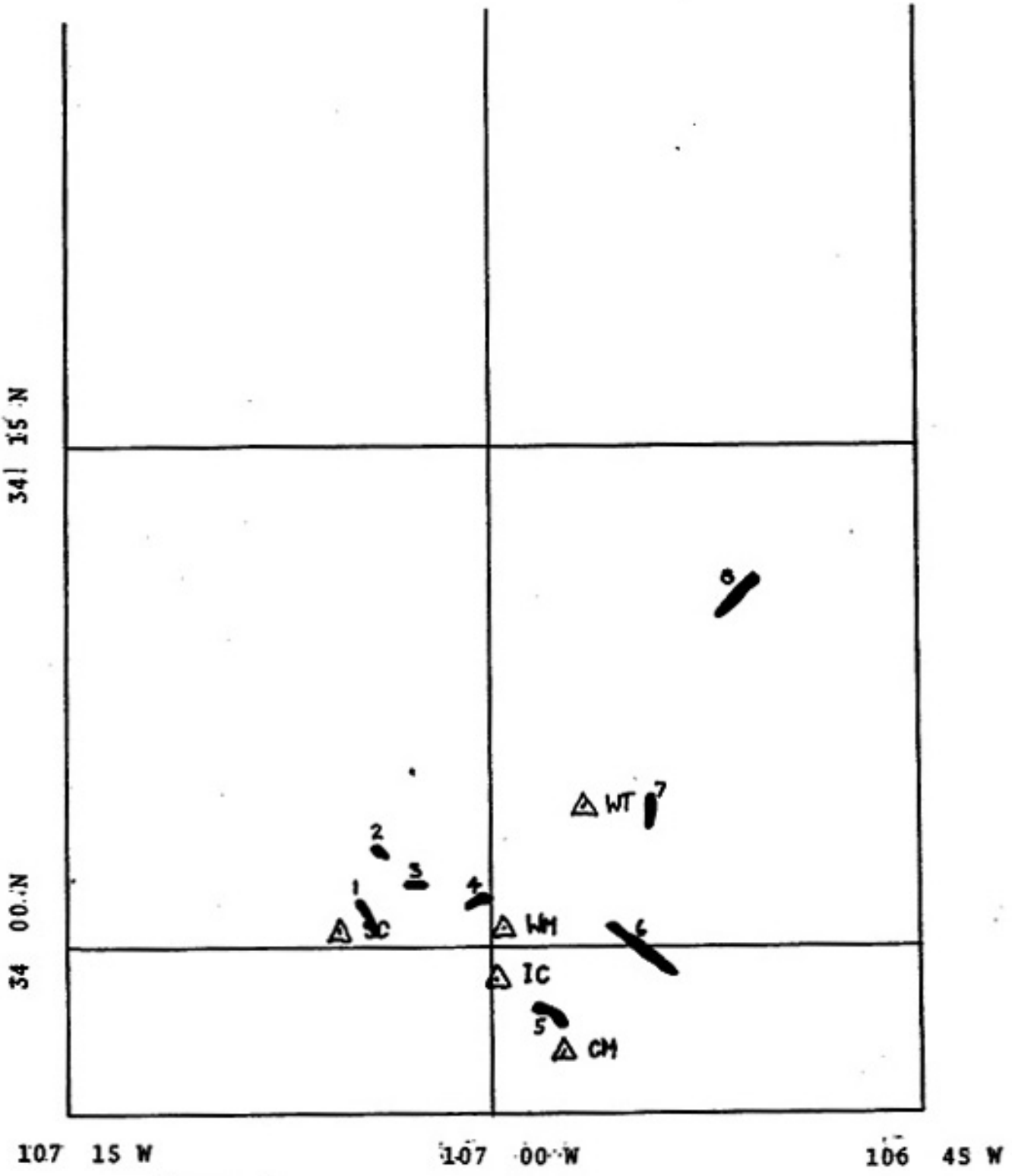

Figure 9.
The positions of the eight proposed anomolous bodies as interpreted by Johnston (1978).

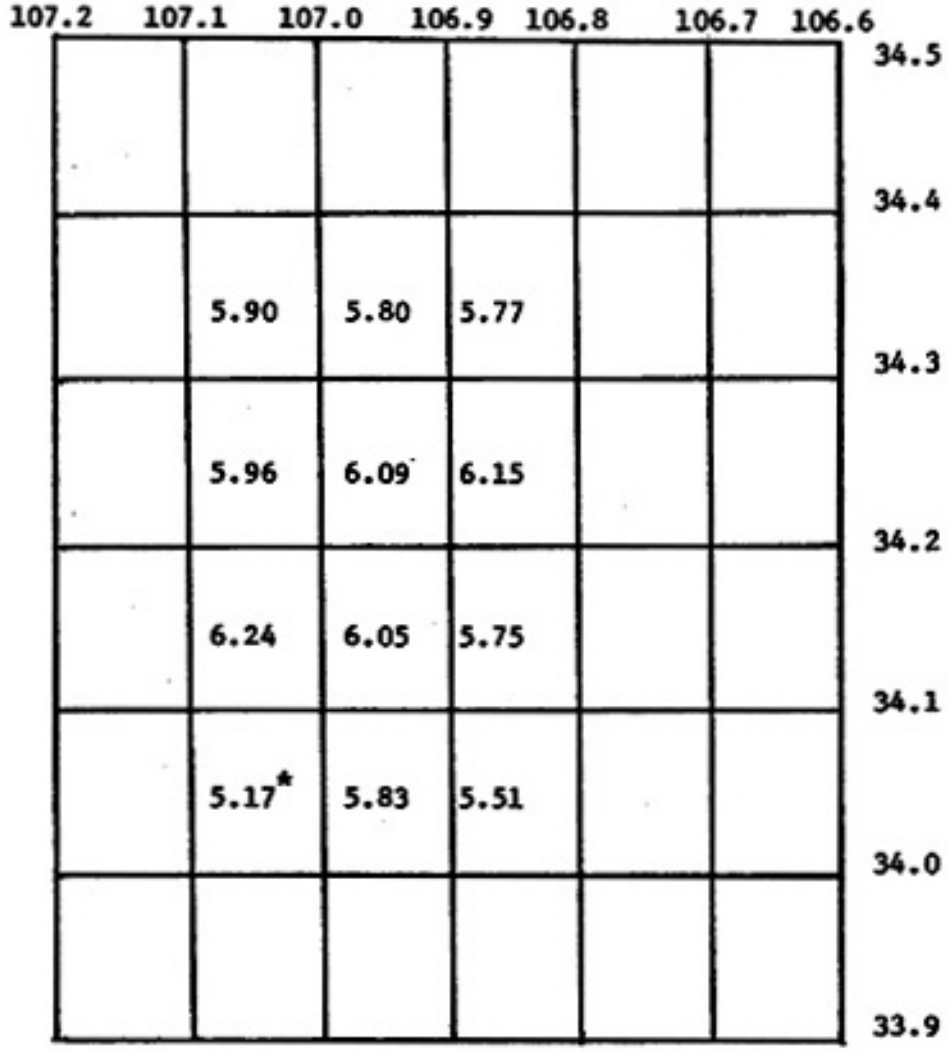

Figure 10.
The final velocity model as interpreted by Ward et al. (1981). Listed are the velocities for each geographical block. Blank regions represent volumes for which velocities were not determined. The top surface of this diagram starts at a depth of 4.0 km. (note: the anomolous region is marked by a *).

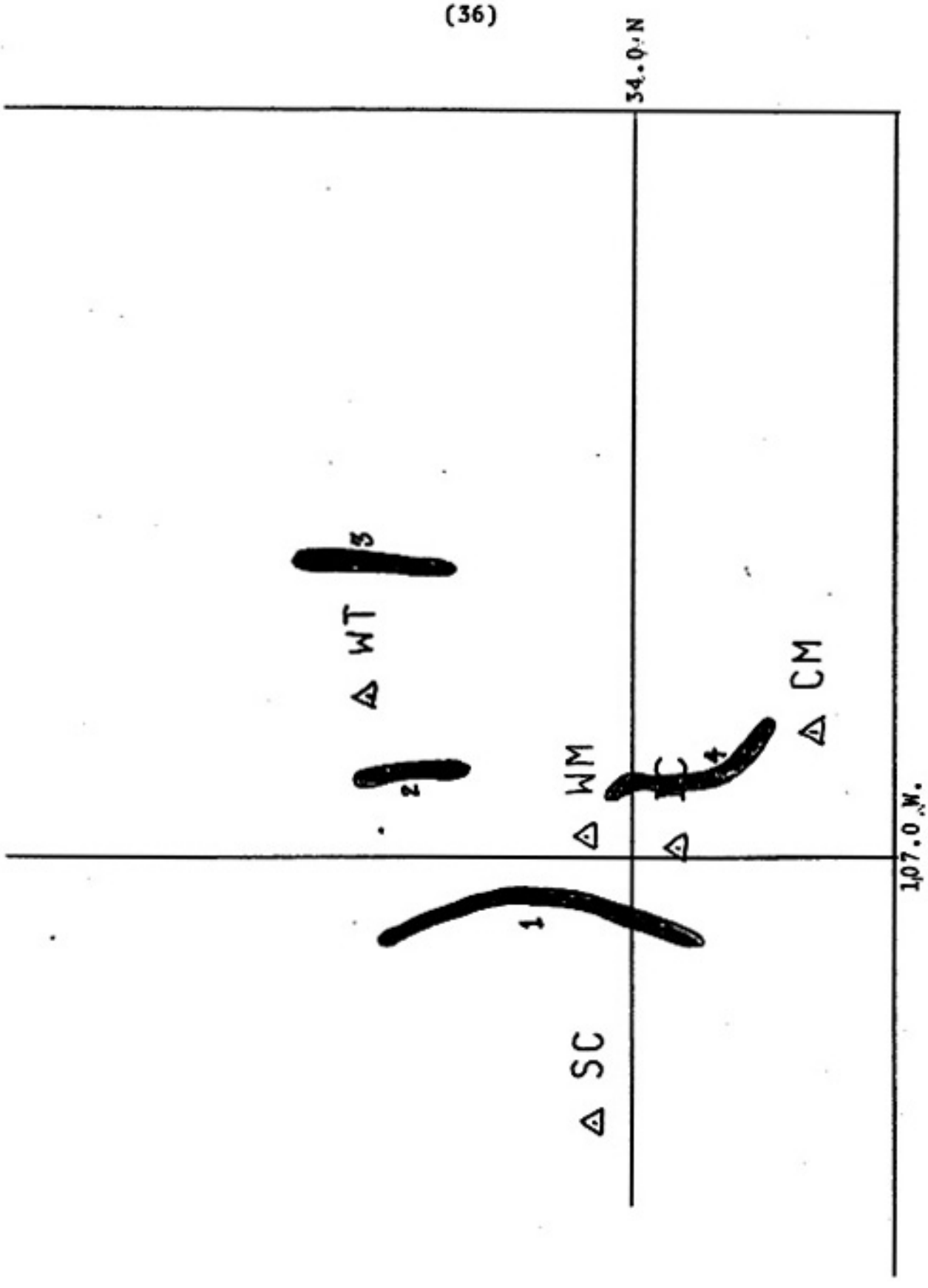

Figure 11.
The proposed anomolous bodies as interpreted by Shuleski (1976) and later modified by Sanford (1977).

the position of their body 3. A match does exist, however, with my proposed area 2 to the central region of their area 4.

In comparing this study with earlier studies, one can see that there does exist differences in shape and shifts in locations of the anomalous crust. These differences may be explained in part by the assumptions made in each study. For this study, the anomalous crustal volumes were placed mid-way between stations to maximize their depths. The position of the bodies can be shifted somewhat and still be compatible with the data. There is also an expected difference between this work and past studies because we now have much higher accuracy in hypocenter location solutions primarily because S as well as P waves were used by Wieder (1981). Differences are also expected because this study was able to use reasonably constrained fault plane solutions not available to earlier studies and a more elaborate and accurate set of corrections.

CONCLUSIONS

In summary, seismic attenuation of the S phase can be used to map areas of magmatic intrusion. In the Rio Grande rift near Socorro, New Mexico three shallow anomalous crustal bodies have been located and reside above the mid-crustal magma body lying at a depth of 19.2 km. The bodies are dike shaped which agrees with the local stress field. They trend in a north-south direction paralleling the rift. The magma in the anomalous crustal areas occurs as intermingled globuals of magma separated by normal rock because along some raypaths S-phase energy is able to pass through without attenuation. It is hoped that with further improvements in the hypocenter location solutions and expanded data sets, volumes of crust containing magma can be located with greater precision.

ACKNOWLEDGEMENTS

I would like to express my deep appreciation to Dr. Allan Sanford for his extreme patience and valuable assistance in this entire project. His manuscript critiques and suggestions have been a great help in the completion of this study.

REFERENCES

Brocher, T. M., Geometry and Physical Properties of the Socorro, New Mexico, Magma Bodies, Jorn. of Geophys. Resear., Vol. 86, No. B10, 9420-9432, Oct. 10, 1981.

Brown, L. D., P. A. Krumhansl, C. E. Chapin, A. R. Sanford, F. A. Cook, S. Kaufman, J. E. Oliver, and F. S. Schilt, COCORP seismic reflection studies of the Rio Grande rift, in Rio Grande Rift: Tectonics and Magmatism, R. E. Riecker, ed., American Geophysical Union, 164-184, 1979.

Brown, L. D., C. E. Chapin, A. R. Sanford, S. Kaufman, and J. E. Oliver, Deep structure of the Rio Grande rift from seismic reflection profiling, J. Geophys. Res., 85, 4773-4800, 1980.

Caravella, F. J., A Study of Poisson's Ratio in the Upper Crust of the Socorro, New Mexico Area., N. Mex. Inst. of Mining and Technol., Geosc. Dept., Geophysics Open-File Report 11, Socorro, 1976.

Chapin, C. E., The Rio Grande rift, Part I: Modifications and additions, N. Mex. Geol. Soc. Field Conf. Guideb., 22, 191-201, 1971.

Chapin, C. E., R. M. Chamberlin, G. R. Osburn, D. W. White and A. R. Sanford, Exploration framework of the Socorro Geothermal Area, New Mexico, Field Guide to Selected Cauldrons and Mining Districts of the Datil-Mogollon Volcanic Field New Mexico, New Mexico Geol. Soc. Special Pub. 7, 114-129, 1978.

Chapin, C. E., and W. R. Seager, Evolution of the Rio Grande rift in the Socorro and Las Cruces area, N. Mex. Geol. Soc. Field Conf. Guideb., 26, 297-321, 1975.

Cordell, L., Regional geophysical setting of the Rio Grande rift, Geol. Soc. Amer. Bull. 89, 1073-1090, 1978.

Fender, J. J., A Study of Poisson's Ratio in the Upper Crust in the Socorro, New Mexico Area., N. Mex. Geophysics Open-File Report, 25, Socorro, 1978.

Frishman, M. S., Use of Linear Inverse Techniques to Study Poisson's Ratio in the Upper Crust in the Socorro, New Mexico Area., N. Mex. Inst. of Mining and Technol., Geosc. Dept., Geophysics Open-File Report, 27, Socorro, 1979.

Hawley, J. W., ed., Guidebook to the Rio Grande rift in New Mexico and Colorado, N. Mex. Bur. of Mines and Miner. Resourc., Cir. 163, 1978.

Johnston, J. A., Microearthquake frequency attenuation of S phases in the Rio Grande rift near Socorro, New Mexico, N. Mex. Inst. of Mining and Technol., Geosc. Dept., Geophysics Open-File Report No. 24, Socorro, 1978.

Julian, B. R., Calculator Program: Earthquake Seismic Radiation Pattern, Shear Fault, Hewlett-Packard Users' Library Program 04839A, 197_.

Lee, W. H. K., and J. C. Lahr, HYPO71 (revised): A computer program for determining hypocenter, magnitude, and first motion pattern of local earthquakes: U. S. Geological Survey, Open-File Report, 75-311, 1975.

Riecker, R. E., ed., Rio Grande Rift: Tectonics and Magmatism, American Geophysical Union, Washington, D. C., 1979.

Rinehart, E. J., A. R. Sanford, and R. M. Ward, Geographic extent and shape of an extensive magma body at midcrustal depths in the Rio Grande rift near Socorro, New Mexico, in Rio Grande Rift: Tectonics and Magmatism, R. E. Riecker, ed., Amer. Geophys. Union, Washington, D. C., 237-251, 1979.

Sanford, A. R. and L. T. Long, Microearthquake crustal reflections, Socorro, New Mexico, Bull. Seism. Soc. Am., 55, 579-586, 1965.

Sanford, A. R., O. S. Alptekin, and T. R. Toppozada, Use of reflection phases on microearthquake seismograms to map an unusual discontinuity beneath the Rio Grande rift, Bull. Seism. Soc. Am., 63, 2021-2034, 1973.

Sanford, A. R., R. P. Mott, Jr., P. J. Shuleski, E. J. Rinehart, F. J. Caravella, R. M. Ward and T. C. Wallace, Geophysical evidence for a magma body in the crust in the vicinity of Socorro, N.M., in Heacock, J. G., ed., The Earth's Crust, Amer. Geophys. Union Monograph 20, 385-403, 1977.

Sanford, A. R., and J. W. Schlue, Seismic exploration for shallow magma bodies in the vicinity of Socorro, New Mexico, New Mexico Energy Institute at New Mexico State University, N.M.E.I., 56, 1980.

Shuleski, P. J., Seismic fault motion and SV wave screening by shallow magma bodies in the vicinity of Socorro, New Mexico, N. Mex. Inst. of Mining and Technol., Geosc. Dept., Geophysics Open-File Report No. 8, Socorro, 1976.

Ward, R. M., Determination of three dimensional velocity anomalies within the upper crust in the vicinity of Socorro, New Mexico using first P arrivals from local earthquakes, Ph.D. dissertation, N. Mex. Inst. of Mining and Technol., Socorro, 1980.

Wieder, D. P., Tectonic Significance of Microearthquake Activity from Composite Fault-Plane Solutions in the Rio Grande Rift Near Socorro, New Mexico, N. Mex. Inst. of Mining and Technol., Geosc. Dept., Open-File Report No. , Socorro, 1981.

Winkler, K. W. and A. Nur, Seismic Attenuation:Effects of Pore Fluids and Frictional Sliding, Geophysics, Soc. of Explor. Geophys., Vol. 47, No. 1, Jan. 1982, 1-15.

APPENDIX I.

The data used for the determination of anomalous behavior. Listed are all events and a designation as to whether the event was found to be anomalous.

DATE	O. T.	LAT.	LONG.	DEP.	ANOM.	STA.	P-AMP.	S-AMP.
06, 03, 75	15:10:15.48	34.02	107.04	10.51	**	SC	17.50	18.50
					**	CM	3.00	4.00
06, 16, 75	23:43:20.82	34.02	107.04	10.64		SC	9.25	6.00
07, 23, 75	14:56:41.82	34.01	107.04	9.93		SC	33.50	8.75
07, 24, 75	17:10:14.16	34.01	107.04	10.31	**	SC	20.50	2.50
07, 30, 75	15:54:15.41	34.08	106.91	9.23		WT	15.00	7.00
07, 30, 75	21:44:42.06	34.08	106.92	9.60		WT	22.50	12.00
08, 05, 75	04:17:20.58	34.02	106.98	10.44		WT	22.50	10.00
						CM	6.50	9.50
					**	SC	17.00	12.50
08, 05, 75	14:19:22.36	34.02	107.04	10.06	**	SC	21.50	19.00
					**	CM	2.25	3.25
						WT	3.25	5.00
08, 06, 75	20:12:33.13	34.02	106.97	8.97	**	WT	4.00	1.50
08, 08, 75	10:53:57.82	34.06	106.92	8.67		CM	6.50	20.00
						SC	6.50	23.00
08, 08, 75	10:57:22.32	34.07	106.92	8.54		WT	9.50	2.50
08, 13, 75	03:38:51.07	34.07	106.92	8.95		CM	27.50	34.00
						SC	9.50	33.00
08, 13, 75	03:46:05.84	34.07	106.92	8.52		WT	7.75	5.00
08, 13, 75	07:39:18.43	34.07	106.93	8.86		WT	16.00	13.50
						CM	5.50	3.50
08, 13, 75	11:22:26.70	34.01	106.97	10.13		CM	10.00	5.00
						SC	5.25	6.00
08, 19, 75	08:11:46.74	34.05	106.96	10.08		WT	9.50	4.00
						SC	3.00	1.50
08, 19, 75	08:12:44.76	34.05	106.96	9.97		WT	9.50	4.00
						SC	3.50	1.50
08, 19, 75	20:10:22.97	34.07	106.92	8.18		WT	5.25	3.50
08, 20, 75	05:16:40.25	34.07	106.90	8.46		CM	32.50	33.00
						SC	16.50	34.00
08, 20, 75	05:22:19.90	34.07	106.92	9.26		CM	34.00	34.00
					**	SC	24.00	34.00

08, 20, 75	12:20:52.20	34.07	106.91	8.18		WT	19.50	9.50
						CM	4.00	5.00
08, 20, 75	12:49:19.27	34.07	106.92	8.57		WT	5.50	5.50
						CM	3.50	2.00
08, 20, 75	15:28:36.29	34.08	106.92	9.47		CM	27.00	33.00
						SC	7.75	25.00
08, 20, 75	21:59:44.60	34.07	106.92	7.80		WT	4.50	3.00
08, 21, 75	00:40:22.93	34.07	106.92	7.45		WT	10.00	7.00
						CM	2.00	2.75
08, 21, 75	03:44:48.60	34.02	107.04	10.08	**	WT	23.50	34.50
					**	CM	7.50	33.50
08, 21, 75	07:03:51.48	34.07	106.91	8.03		WT	24.00	21.00
						CM	12.00	18.00
						SC	3.00	9.50
08, 21, 75	19:04:06.18	34.04	106.96	10.05		WT	9.50	4.00
						SC	4.50	2.00
08, 21, 75	19:09:11.54	34.05	106.96	10.67		WT	23.50	18.00
						CM	6.25	20.00
						SC	15.50	8.00
08, 21, 75	19:18:42.12	34.04	106.96	9.82		WT	22.50	15.00
						CM	4.50	18.00
						SC	13.50	6.50
08, 25, 75	19:37:40.85	34.07	106.92	9.03		WT	13.00	10.00
						CM	7.25	6.50
08, 26, 75	08:40:15.73	34.07	106.92	9.45		WT	8.00	3.25
08, 28, 75	01:26:02.40	34.07	106.92	8.28		WT	4.00	3.00
08, 29, 75	03:17:35.53	34.08	106.92	8.36		WT	9.25	7.00
						CM	3.25	3.50
08, 29, 75	03:18:09.46	34.07	106.93	8.35		WT	7.25	4.00
08, 29, 75	08:52:18.85	34.08	106.93	7.80		WT	21.00	12.50
						CM	5.00	7.50
09, 16, 75	13:30:52.46	34.08	106.93	7.74		WT	25.75	25.00
						CM	14.50	14.25
09, 24, 75	02:17:09.44	34.05	106.93	8.28		WT	4.75	4.00
09, 24, 75	13:16:40.52	34.06	106.93	7.70		WT	19.50	10.00

10, 30, 75	07:09:38.56	34.02	107.03	10.88	**	SC	8.00	6.50
						CM	2.00	1.25
11, 04, 75	16:30:11.68	34.04	107.07	9.77		SC	2.50	25.00
11, 05, 75	14:35:05.11	34.03	107.07	10.19		SC	11.50	28.00
					**	WT	3.25	9.00
						CM	7.25	9.00
11, 06, 75	08:24:48.04	34.03	107.01	10.09		SC	3.00	3.00
11, 06, 75	09:33:58.89	34.03	107.01	10.37		SC	4.25	5.00
01, 22, 76	16:00:52.31	34.04	107.04	9.54	**	WT	33.00	37.00
01, 22, 76	16:05:11.00	34.03	107.04	11.52	**	SC	32.00	30.00
					**	WT	10.00	34.00
						CM	7.00	23.50
01, 23, 76	02:53:33.03	34.03	107.03	8.98	**	SC	12.25	30.00
						WT	8.50	23.25
					**	CM	8.50	14.00
01, 23, 76	08:16:19.25	34.03	107.04	10.06	**	SC	5.25	18.50
					**	CM	4.00	7.00
01, 29, 76	15:06:40.19	33.98	106.97	7.00	**	WT	14.00	26.50
						SC	31.50	32.00
01, 29, 76	18:24:27.51	33.98	106.98	7.52		CM	7.50	3.50
						SC	4.00	3.00
01, 30, 76	09:16:35.44	33.98	106.98	8.35		CM	3.00	1.50
						SC	3.00	2.00
02, 17, 76	06:17:48.98	34.03	107.06	10.69		SC	3.50	12.50
02, 17, 76	17:34:05.15	34.04	107.00	10.82		WM	5.00	6.50
						WT	14.00	24.75
						IC	17.50	7.25
02, 18, 76	05:44:55.92	34.01	107.05	10.27		WM	2.75	1.00
02, 19, 76	00:08:36.81	34.02	107.06	9.92		SC	10.00	27.00
						IC	9.00	7.00
						CM	3.00	5.50
02, 20, 76	12:51:45.11	34.01	107.04	11.11	**	WM	5.00	1.75
03, 25, 76	10:50:54.07	34.05	106.97	10.26		WT	7.50	3.50
04, 13, 76	09:45:40.75	34.06	107.01	8.59		WM	8.00	5.75
						WT	2.00	4.25
04, 13, 76	11:17:05.09	34.06	107.01	8.04		WM	2.25	1.50

04,13,76	11:41:25.36	34.03	107.06	10.52		WM	2.50	1.00
04,13,76	11:58:34.64	33.98	106.96	6.41	**	IC	14.25	9.00
						CM	7.00	7.50
					**	WM	19.00	15.00
					**	WT	3.25	8.00
04,14,76	01:50:28.88	33.98	107.00	9.80	**	IC	3.00	2.25
					**	WM	2.75	4.50
						SC	2.50	3.50
04,15,76	03:41:48.76	34.06	107.00	9.40		WM	3.75	3.00
04,15,76	08:45:52.51	34.06	107.01	8.58		WM	5.75	4.75
04,15,76	08:51:50.64	34.06	107.02	7.72		WM	2.00	2.75
04,15,76	10:24:12.82	34.06	107.01	7.69		WM	3.75	2.75
04,15,76	11:55:20.07	34.06	107.01	7.69		WM	5.00	4.00
04,15,76	15:30:27.48	34.06	107.02	8.07		WM	3.50	2.75
04,15,76	18:28:37.23	34.05	106.95	7.95		WT	2.00	2.50
04,15,76	22:48:20.64	34.05	106.96	8.28		IC	2.00	2.25
04,15,76	23:16:11.87	34.06	107.01	7.56		WM	2.00	1.50
04,16,76	01:20:22.71	34.06	107.02	7.90		WM	2.50	2.25
04,16,76	09:33:42.88	34.06	107.01	7.58		WM	31.00	29.50
						IC	26.50	34.00
					**	SC	18.00	20.50
						CM	6.50	9.25
04,16,76	09:36:07.88	34.06	107.02	6.65		WM	3.75	3.25
04,16,76	14:07:33.22	34.07	106.99	8.97		IC	16.00	34.50
					**	SC	25.00	22.50
						CM	2.00	14.00
04,16,76	15:04:36.66	34.06	107.02	7.73		WM	2.00	4.50
					**	WT	2.00	2.50
06,08,76	06:16:12.41	34.04	107.00	10.37		WT	2.25	2.00
					**	SC	2.50	3.00
06,30,76	08:44:01.50	34.01	107.03	10.61		SC	2.50	2.00
					**	WT	3.00	3.00
07,15,76	16:43:07.66	34.02	107.06	11.08		SC	4.00	26.00
						WT	2.25	11.00

08,09,76	18:40:17.60	34.05	107.00	9.58	**	WT	6.25	4.50
						SC	6.75	6.25
08,09,76	22:27:39.19	34.04	107.00	10.89	**	WT	3.50	2.50
						SC	3.25	3.25
08,10,76	02:53:11.52	34.05	107.00	10.26	**	WT	8.50	5.50
						SC	8.50	8.00
08,10,76	04:38:25.39	34.02	107.06	9.90		SC	3.00	8.00
08,10,76	12:18:41.77	34.05	106.99	11.09	**	WT	14.50	9.50
						SC	16.50	15.50
08,11,76	06:03:43.56	34.06	107.00	9.17	**	WT	3.00	2.00
						SC	2.75	2.50
08,12,76	00:59:08.01	34.04	107.00	11.33	**	WT	12.00	7.50
						SC	5.50	10.50
08,12,76	01:54:04.77	34.04	107.00	9.74		WT	10.00	10.50
						SC	6.00	13.00
08,12,76	02:34:25.87	34.04	107.00	10.37	**	WT	9.00	5.50
						SC	6.50	8.25
08,12,76	04:56:05.06	34.05	107.00	11.67	**	WT	29.00	29.00
						SC	23.00	31.50
08,12,76	05:08:59.07	34.05	107.00	10.63	**	WT	2.00	2.00
						SC	2.25	2.50
08,12,76	05:20:48.69	34.05	107.00	10.24	**	WT	4.00	2.50
						SC	3.50	4.50
08,12,76	07:52:06.31	34.05	107.00	9.75	**	WT	33.00	34.50
						SC	32.00	33.00
08,12,76	11:25:51.57	34.04	107.00	10.00	**	WT	7.00	5.00
						SC	5.00	7.50
08,12,76	23:07:12.52	34.05	107.00	10.60		WT	21.00	15.00
08,13,76	03:07:42.23	34.04	107.00	9.38	**	WT	5.50	3.50
08,25,76	21:04:09.33	34.05	107.00	10.85	**	SC	2.00	1.50
08,25,76	22:32:23.10	34.05	107.00	11.57	**	WT	2.00	0.75
						SC	2.00	1.75
08,27,76	08:15:28.15	34.01	107.06	10.81		SC	10.50	5.00
08,27,76	10:42:33.60	34.01	107.05	11.16		SC	7.00	4.50
09,03,76	06:45:56.23	33.97	106.98	9.29	**	SC	3.25	0.50

09,03,76	06:46:29.32	33.97	106.98	9.60	**	SC	9.00	4.00
09,03,76	13:25:58.17	33.99	106.97	11.71	**	WT	3.25	2.00
						SC	2.50	2.75
10,05,76	19:26:08.65	34.04	106.96	10.14		WT	5.50	2.00
						SC	2.50	1.25
10,07,76	22:35:49.40	34.02	107.03	11.16		IC	3.75	3.00
					**	SC	2.50	6.00
10,07,76	22:37:37.66	34.03	107.03	10.36		IC	11.50	9.00
						SC	3.00	14.00
10,07,76	23:21:09.59	34.02	107.03	10.24		IC	9.25	6.75
						SC	3.00	14.00
01,21,77	16:38:11.38	34.01	107.06	9.16	**	CM	32.50	33.00
						WT	3.00	34.50
01,21,77	16:42:28.36	34.01	107.06	11.03		SC	2.50	9.00
01,21,77	16:43:39.84	34.01	107.05	10.33		CM	18.75	35.50
					**	WT	3.25	23.00
01,22,77	04:24:05.02	34.01	107.05	9.64		SC	5.25	10.00
02,08,77	21:15:58.47	34.03	107.04	10.73		SC	5.25	2.50
02,09,77	01:36:16.12	34.02	107.04	10.70		SC	9.00	4.25
02,09,77	08:38:47.31	33.99	106.97	8.03		CM	2.00	9.00
02,09,77	10:59:58.84	34.02	107.00	7.04		CM	15.00	13.00
					**	SC	23.00	9.50
02,09,77	11:07:13.69	34.01	107.00	9.80	**	CM	2.25	2.00
					**	SC	3.00	2.00
02,09,77	12:26:35.17	34.03	107.04	10.59		SC	5.25	2.50
02,11,77	08:28:03.38	33.99	106.97	12.11		CM	5.00	9.25
02,11,77	08:31:45.49	33.99	106.97	12.13		CM	4.00	5.00
02,16,77	08:51:16.69	34.02	107.05	10.30		SC	2.00	5.57
						IC	4.00	2.75
02,16,77	14:44:49.47	34.01	107.05	9.91		IC	5.00	2.50
						CM	2.00	3.75
02,25,77	00:07:08.07	34.01	107.05	10.27	**	SC	3.50	11.00
						IC	9.50	7.00

03,08,77	04:30:41.64	34.00	107.06	10.40		SC	3.50	11.25
03,08,77	04:55:06.07	34.01	107.05	9.71		SC	3.50	4.25
03,09,77	11:25:44.37	34.01	107.05	9.87		SC	22.50	23.00
					**	WT	3.00	6.00
03,09,77	11:49:02.43	34.01	107.06	9.59		SC	37.00	38.00
						CM	6.00	30.00
					**	WT	5.00	21.00
03,09,77	11:50:15.93	34.01	107.06	9.39		SC	33.00	34.50
						CM	11.00	34.50
					**	WT	9.50	27.00
03,09,77	12:27:55.97	34.01	107.05	10.00		SC	20.00	29.50
						CM	2.00	8.00
					**	WT	2.00	7.00
03,09,77	12:33:19.15	34.01	107.05	9.35		SC	3.25	6.50
03,09,77	12:39:00.20	34.01	107.05	9.71		SC	5.50	6.50
03,10,77	01:29:50.07	34.03	107.07	10.64		SC	2.00	13.00
03,10,77	02:03:42.59	34.00	107.06	10.18		SC	5.50	16.00
						CM	2.00	3.50
04,05,77	19:34:30.76	34.00	107.05	12.08		SC	8.00	5.50
04,27,77	12:15:56.25	34.01	107.05	9.81		SC	3.25	20.00
04,27,77	12:23:27.19	34.02	107.06	10.20		SC	9.75	35.50
						CM	5.50	8.50
04,28,77	10:59:10.49	34.04	107.05	9.68	**	SC	4.50	22.25
						WT	2.00	11.75
06,01,77	06:40:44.85	34.01	107.06	9.53		CM	10.00	16.00
06,02,77	06:45:50.56	34.01	107.07	9.11		SC	2.25	24.00
06,02,77	06:50:24.36	34.01	107.06	8.99		SC	8.00	16.25
						CM	12.50	28.50
					**	WT	5.00	20.00
06,02,77	06:55:21.42	34.01	107.06	8.22		SC	28.50	28.00
06,02,77	08:11:47.68	34.01	107.06	7.00		SC	4.00	21.00
06,02,77	11:42:00.47	34.01	107.06	7.73		SC	8.50	24.25
06,02,77	12:07:04.04	34.01	107.06	7.83		SC	2.00	24.50
06,02,77	14:29:06.71	34.01	107.06	7.94		SC	18.50	25.50

06,02,77	17:30:08.17	34.01	107.06	8.24		SC	30.00	27.00
06,03,77	03:49:01.56	34.01	107.06	8.77		SC	13.25	28.00
						CM	3.50	9.00
06,03,77	20:45:03.28	34.23	106.90	7.00		WT	2.50	7.50
						CM	4.00	15.00
06,10,77	04:04:44.84	34.02	107.06	9.96		SC	5.25	31.50
						CM	4.25	12.50
07,15,77	12:26:25.70	34.01	107.06	10.04		SC	15.50	31.00
						CM	12.50	21.50
					**	WT	2.50	24.25
07,21,77	17:40:14.11	34.01	107.06	10.41		SC	2.50	8.00
07,27,77	15:53:15.04	34.01	107.06	10.93		SC	2.25	8.25
07,27,77	18:08:20.17	34.16	106.91	6.66		SC	2.50	9.50
08,17,77	06:03:19.88	34.16	106.86	7.40		CM	3.00	6.50
08,18,77	10:38:14.82	34.02	107.06	9.21	**	WT	5.75	25.25
08,18,77	10:38:47.51	34.01	107.06	10.31		SC	8.00	26.50
						CM	3.50	9.00
					**	WT	2.25	16.00
08,18,77	10:39:09.87	34.01	107.06	10.57		CM	14.00	24.50
08,18,77	12:16:45.02	34.01	107.06	10.33		SC	2.00	13.00
08,19,77	03:51:00.22	34.02	107.06	8.52		SC	27.00	33.00
						CM	6.00	15.00
					**	WT	7.25	25.50
08,19,77	09:05:48.23	34.01	107.06	10.40		SC	3.00	7.00
08,19,77	09:27:07.49	34.00	107.07	10.84		SC	4.00	1.75
08,19,77	09:28:22.66	34.01	107.07	11.39		SC	27.50	12.50
						CM	2.75	11.50
08,19,77	09:49:51.09	34.01	107.06	10.04		SC	2.25	3.50
08,19,77	10:24:42.59	34.01	107.06	10.22		SC	14.00	12.50
08,24,77	11:22:35.67	34.01	107.06	10.57		CM	4.50	9.00
08,25,77	04:52:32.76	33.95	106.96	8.15		CM	25.00	17.00
						SC	4.00	5.75
08,25,77	06:26:26.99	34.01	107.06	9.77		SC	14.50	33.50

						CM	3.50	12.50
					**	WT	3.50	24.50
09,01,77	21:58:48.52	34.01	107.05	10.21	**	SC	31.5 0	16.50
					**	CM	2.25	16.50
					**	WT	19.50	24.25
09,02,77	07:41:11.71	33.98	107.00	6.55		CM	5.75	4.00
						SC	5.00	4.00
09,14,77	04:01:27.66	34.04	107.03	7.04		SC	11.00	10.50
09,15,77	00:53:35.23	34.03	107.06	10.06		SC	8.00	33.50
09,20,77	08:19:23.18	34.16	106.87	7.21		WT	2.25	4.00

APPENDIX II.

COMPOSITE FAULT-PLANE AREA		AZIMUTH	PLUNGE	WELL CONSTRAINED SOLUTIONS
1	a	254.0	-50.0	**
	n	257.0	40.0	**
2	a	77.0	-52.0	**
	n	84.0	37.0	**
3	a	232.0	-44.0	**
	n	243.0	46.0	**
4	a	206.0	-42.0	
	n	256.0	36.0	
5	a	263.0	-44.0	
	n	292.0	42.0	
6	a	86.0	-54.0	**
	n	86.0	36.0	**
7	a	84.0	-74.0	**
	n	22.0	16.0	**
8	a	234.0	-52.0	**
	n	275.0	30.0	**
9	a	222.0	-52.0	
	n	278.0	24.0	
10	a	229.0	-50.0	
	n	256.0	36.0	
11	a	268.0	-54.0	**
	n	260.0	36.0	**
12	a	218.0	-47.0	
	n	279.0	24.0	

A Listing of the fault plane solutions from 12 distinct geographic areas as deduced by Wieder (1981) and used in the calculation of theoretical ratios.

APPENDIX III.

The three programs used in drawing the raypaths in areal, N-S cross-sectional, and E-W cross-sectional views. They are in standard Fortran and have used the Plotl0 subroutine library.

```
C**********************************************************************
C * THIS IS A PLOTTING PROGRAM USING THE PLOT10 SUBROUTINE LIBRARY.    *
C * THE PROGRAM WILL PLOT A LOCAL MAP WITH CROSS MARKS AT 0.1 DEGREE   *
C * POINTS. THE LOCATION OF THE STATION NAMED IN THE PROGRAM TITLE     *
C * (MT IN THIS CASE) WILL BE SHOWN ALONG WITH THE STATION NAME.       *
C * FOLLOWING THIS, A PLOT OF ALL THE ANOMALOUS RAYPATHS TO THIS       *
C * STATION WILL APPEAR.                                               *
C**********************************************************************

      INTEGER FLAG,NAME(2),CROSS(1)
      INTEGER LAT1(4),LAT2(4),LAT3(4),LAT4(4),LAT5(4)
      INTEGER LONG1(5),LONG2(5),LONG3(5),LONG4(5)
      REAL RAY1(1000,3)
      OPEN(UNIT=7,DEVICE='DSK',ACCESS='SEQIN',FILE='RAYT')
C
C SET THE SYMBOL DESIGNATION FOR PLOT10 FORMAT
C
      LAT1(1)=51
      LAT1(2)=51
      LAT3(1)=51
      LAT3(1)=51
      LAT4(1)=51
      LAT5(1)=51
      LAT5(4)=51
      LAT1(3)=46
      LAT2(3)=46
      LAT3(3)=46
      LAT4(3)=46
      LAT5(3)=46
      LAT1(4)=57
      LAT2(2)=52
      LAT3(2)=52
      LAT4(2)=52
      LAT5(2)=52
      LAT2(4)=48
      LAT3(4)=49
      LAT4(4)=50
      LONG1(1)=49
      LONG1(5)=49
      LONG2(1)=49
      LONG3(1)=49
      LONG4(1)=49
      LONG1(2)=48
      LONG2(2)=48
      LONG2(5)=48
      LONG3(2)=48
      LONG4(2)=48
      LONG1(3)=55
      LONG2(3)=55
      LONG1(4)=46
      LONG2(4)=46
      LONG3(4)=46
      LONG4(4)=46
      LONG3(3)=54
      LONG4(3)=54
      LONG3(5)=57
      LONG4(5)=56
      FLAG=0
C
C READ IN THE LIST OF ANOMALOUS EVENTS TO BE PLOTTED
C
      DO 200 I=1,1000
      READ(7,F.0=200,100)(RAY1(I,J),J=1,2)
100   FORMAT(F5.2,1X,F7.2,1X,F6.2)
      FLAG=FLAG+1
200   CONTINUE
      CROSS(1)=43
      CALL INITT(400)
C
C MARK THE MARGIN OF THE MAP
C
      Y=33.90
      X=-107.10
115   CALL MOVEA(X,Y)
      CALL ANSTR(1,CROSS)
      X=X+.10
      IF(X.GT.-106.70)GO TO 700
      GO TO 115
700   Y=Y+.10
      IF(Y.GT.34.20)GO TO 701
      X=-107.10
      GO TO 115
701   CALL ANNODE
      ACCEPT 569,A
569   FORMAT(F)
      CALL MOVEA(-107.12,34.26)
      CALL ANSTR(5,LONG1)
      CALL MOVEA(-107.02,34.26)
      CALL ANSTR(5,LONG2)
      CALL MOVEA(-106.92,34.26)
      CALL ANSTR(5,LONG3)
      CALL MOVEA(-106.82,34.26)
      CALL ANSTR(5,LONG4)
      CALL MOVEA(-106.75,33.90)
      CALL ANSTR(4,LAT1)
      CALL MOVEA(-106.75,34.00)
      CALL ANSTR(4,LAT2)
      CALL MOVEA(-106.75,34.10)
      CALL ANSTR(4,LAT3)
      CALL MOVEA(-106.75,34.20)
      CALL ANSTR(4,LAT4)
      CALL POINTA(-106.95,34.07)
      CALL MOVEA(-106.94,34.06)
      NAME(1)=87
      NAME(2)=84
      CALL ANSTR(2,NAME)
C
C FIND LOCATION OF ANOMOLOUS EPICENTER AND DRAW RAYPATH TO IT FROM
C STATION COORDINATE
C
402   CALL MOVEA(-106.95,34.07)
      K=1
714   X=RAY1(K,1)
      Y=RAY1(K,2)
      CALL DRAWA(X,Y)
      CALL MOVEA(-106.95,34.07)
      K=K+1
      IF(K.GT.FLAG)GO TO 715
      GO TO 714


715   CALL ANNODE
      ACCEPT 899,A
899   FORMAT(F)
      STOP
      END
```

(55)

```
C*****************************************************************
C* THIS IS A PROGRAM USING IPL PLOT10 SUBROUTINE LIBRARY.        *
C* THE PROGRAM WILL PLOT A CROSS SECTIONAL MAP OF LATITUDE       *
C* AND DEPTH. THE LATITUDE WILL BE MARKED AT 0.1 DEGREE          *
C* INTERVALS AND DEPTH WILL BE MARKED AT 5.00 KM LEVELS. THE     *
C* LOCATION OF THE STATIONS USED IN THIS STUDY WILL BE SHOWN     *
C* ALONG WITH THE STATION NAMES. FOLLOWING THIS, A PLOT OF ALL   *
C* THE ANOMOLOUS RAYPATHS TO THIS STATION WILL APPEAR.           *
C*****************************************************************
      INTEGER FLAG,CROSS(1),NT(2),NN(2),SC(2),IC(2),CN(2)
      INTEGER LAT1(4),LAT2(4),LAT3(4),LAT4(4),LAT5(4)
      INTEGER DEP1(3),DEP2(3),DEP3(3),DEP4(3),MARK(1)
      REAL RAY(1000,3)
      OPEN(UNIT=7,DEVICE='DSK',ACCESS='SEQIN',FILE='RAY')
C
C SET THE SYMBOL DESIGNATION FOR PLOT10 FORMAT
C
      LAT1(1)=51
      LAT1(2)=52
      LAT1(3)=46
      LAT1(4)=51
      LAT2(1)=51
      LAT2(2)=52
      LAT2(3)=46
      LAT2(4)=50
      LAT3(1)=51
      LAT3(2)=52
      LAT3(3)=46
      LAT3(4)=49
      LAT4(1)=51
      LAT4(2)=52
      LAT4(3)=46
      LAT4(4)=48
      LAT5(1)=51
      LAT5(2)=51
      LAT5(3)=46
      LAT5(4)=57
      DEP1(1)=48
      DEP1(2)=46
      DEP1(3)=48
      DEP2(1)=53
      DEP2(2)=46
      DEP2(3)=48
      DEP3(1)=49
      DEP3(2)=48
      DEP3(3)=46
      DEP3(4)=48
      DEP4(1)=49
      DEP4(2)=53
      DEP4(3)=46
      DEP4(4)=48
      NT(1)=87
      NT(2)=84
      NN(1)=87
      NN(2)=77
      SC(1)=83
      SC(2)=67
      IC(1)=73
      IC(2)=67
      CN(1)=67
      CN(2)=77
      FLAG=0
C
C READ THE LIST OF ANOMOLOUS EVENTS TO BE PLOTTED
C
      DO 200 I=1,1000
      READ(7,END=200,100)(RAY(I,J),J=1,3)
100   FORMAT(F5.2,1X,F7.2,1X,F6.2)
      FLAG=FLAG+1
200   CONTINUE
      CROSS(1)=108
      MARK(1)=94
      CALL MOVEA(34.32,-10.00)
      CALL ANSTR(3,DEP3)
      CALL MOVEA(34.32,-15.00)
      CALL ANSTR(4,DEP4)
      CALL ANMODE
      ACCEPT 514,B
514   FORMAT(F)
      CALL MOVEA(34.07,0.00)
      CALL ANSTR(1,MARK)
      CALL MOVEA(34.01,0.00)
      CALL ANSTR(1,MARK)
      CALL MOVEA(33.95,0.00)
      CALL ANSTR(1,MARK)
      CALL MOVEA(33.99,0.00)
      CALL ANSTR(1,MARK)
      CALL MOVEA(34.01,0.00)
      CALL ANSTR(1,MARK)
C
C PLOT THE LOCATIONS OF THE STATIONS USED IN THIS STUDY
C
      CALL MOVEA(34.07,0.30)
      CALL ANSTR(2,NT)
      CALL MOVEA(34.01,0.30)
      CALL ANSTR(2,SC)
      CALL MOVEA(33.95,0.30)
      CALL ANSTR(2,CN)
      CALL MOVEA(33.99,0.30)
      CALL ANSTR(2,IC)
      CALL MOVEA(34.01,0.30)
      CALL ANSTR(2,NN)
      CALL MOVEA(34.07,0.00)
      K=1
C
C FIND LOCATIONS OF ANOMOLOUS HYPOCENTERS AND DRAW RAYPATHS TO THEM
C FROM THE STATION COORDINATES
C
714   X=RAY(K,1)
      Y=RAY(K,3)
      CALL DRAWA(X,Y)
      CALL MOVEA(34.07,0.00)
      K=K+1
      IF(K.GT.FLAG)GO TO 715
      GO TO 714
715   CALL ANMODE
      ACCEPT 555,C
555   FORMAT(F)
      STOP
      END
C
C DRAW THE OUTLINE OF THE CROSS SECTIONAL MAP
C
```

```
      CALL INIT3(480)
      CALL DWINDU(33.83,34.38,-15.00,3.00)
      CALL MOVEA(34.30,0.00)
      CALL DRAWA(33.90,0.00)
      CALL DRAWA(33.90,-15.00)
      CALL DRAWA(34.30,-15.00)
      CALL DRAWA(34.30,0.00)
      CALL MOVEA(34.30,0.00)
      CALL ANSTR(1,CROSS)
      CALL MOVEA(34.20,0.00)
      CALL ANSTR(1,CROSS)
      CALL MOVEA(34.10,0.00)
      CALL ANSTR(1,CROSS)
      CALL MOVEA(34.00,0.00)
      CALL ANSTR(1,CROSS)
      CALL MOVEA(33.90,0.00)
      CALL ANSTR(1,CROSS)
      CALL ANMODE
      ACCEPT 666,C
666   FORMAT(F)
      CALL MOVEA(34.30,-5.00)
      CALL DASHA(33.90,-5.00,3)
      CALL MOVEA(33.90,-10.00)
      CALL DASHA(34.30,-10.00,3)
      CALL ANMODE
      ACCEPT 589,A
589   FORMAT(F)
C
C MARK THE MARGIN OF THE MAP
C
      CALL MOVEA(33.84,1.00)
      CALL ANSTP(4,LAT1)
      CALL MOVEA(33.99,1.00)
      CALL ANSTR(4,LAT2)
      CALL MOVEA(34.09,1.00)
      CALL ANSTR(4,LAT3)
      CALL MOVEA(34.19,1.00)
      CALL ANSTR(4,LAT4)
      CALL MOVEA(34.29,1.00)
      CALL ANSTR(4,LAT5)
      CALL MOVEA(34.32,0.00)
      CALL ANSTR(3,DEP1)
      CALL MOVEA(34.32,-5.00)
      CALL ANSTR(3,DEP2)
```

```
*****************************************************************
* THIS IS A PROGRAM USING THE PLOT10 SUBROUTINE LIBRARY.        *
* THE PROGRAM WILL PLOT A CROSS SECTIONAL MAP OF LONGITUDE      *
* AND DEPTH. THE LONGITUDE WILL BE MARKED AT 0.1 DEGREE         *
* INTERVALS AND DEPTH WILL BE MARKED AT 5.00 Km LEVELS.         *
* THE LOCATION OF THE STATIONS USED IN THIS STUDY WILL BE       *
* SHOWN ALONG WITH THE STATION NAMES. FOLLOWING THIS, A         *
* PLOT OF ALL THE ANOMALOUS RAYPATHS TO THIS STATION WILL       *
* APPEAR.                                                       *
*****************************************************************

      INTEGER FLAG,CROSS(1),MT(2),MM(2),SC(2),IC(2),CM(2)
      INTEGER LONG1(5),LONG2(5),LONG3(5),LONG4(5)
      INTEGER DEP1(3),DEP2(3),DEP3(3),DEP4(3),MARK(1)
      REAL RAWAT(1000,3)
      OPEN(UNIT=8,DEVICE='DSK',ACCESS='SLOIN',FILE='RAWT')
C
C SET THE SYMBOL DESIGNATION FOR PLOT10 FORMAT
C
      LONG1(1)=49
      LONG1(2)=48
      LONG1(3)=55
      LONG1(4)=46
      LONG1(5)=49
      LONG2(1)=49
      LONG2(2)=48
      LONG2(3)=55
      LONG2(4)=46
      LONG2(5)=48
      LONG3(1)=49
      LONG3(2)=48
      LONG3(3)=54
      LONG3(4)=46
      LONG3(5)=57
      LONG4(1)=49
      LONG4(2)=48
      LONG4(3)=54
      LONG4(4)=46
      LONG4(5)=56
      DEP1(1)=48
      DEP1(2)=46
      DEP1(3)=48
      DEP2(1)=53
      DEP2(2)=46
      DEP2(3)=48
      DEP3(1)=49
      DEP3(2)=48
      DEP3(3)=46
      DEP3(4)=48
      DEP4(1)=49
      DEP4(2)=53
      DEP4(3)=46
      DEP4(4)=48
      MT(1)=87
      MT(2)=84
      MM(1)=87
      MM(2)=77
      SC(1)=83
      SC(2)=67
      IC(1)=73
      IC(2)=67
      CM(1)=67
      CM(2)=77
      FLAG=0
C
C READ THE LIST OF ANOMALOUS EVENTS TO BE PLOTTED
C
      DO 200 I=1,1000
      READ(7,END=200,100)(RAWT(I,J),J=1,3)
100   FORMAT(F5.2,1X,F7.2,1X,F6.2)
      FLAG=FLAG+1
200   CONTINUE
      CROSS(1)=109
      MARK(1)=94
C
C DRAW THE OUTLINE OF THE CROSS SECTIONAL MAP
C
      CALL INITT(480)
      CALL DWINDO(-107.15,-106.75,-15.00,3.00)
      CALL MOVEA(-107.10,0.00)
      CALL DRAWA(-106.80,0.00)
      CALL DRAWA(-106.80,-15.00)
      CALL DRAWA(-107.10,-15.00)
      CALL DRAWA(-107.10,0.00)
      CALL MOVEA(-107.10,0.00)
      CALL ANSTR(1,CROSS)
      CALL MOVEA(-107.00,0.00)
      CALL ANSTR(1,CROSS)
      CALL MOVEA(-106.90,0.00)
      CALL ANSTR(1,CROSS)
      CALL MOVEA(-106.80,0.00)
      CALL ANSTR(1,CROSS)
      CALL MOVEA(-106.80,-5.00)
      CALL DASHA(-107.10,-5.00,3)
      CALL MOVEA(-106.80,-10.00)
      CALL DASHA(-107.10,-10.00,3)
      CALL ANNODE
      ACCEPT 589,A
589   FORMAT(F)
C
C MARK THE MARGIN OF THE MAP
C
      CALL MOVEA(-107.11,1.00)
      CALL ANSTR(5,LONG1)
      CALL MOVEA(-107.01,1.00)
      CALL ANSTR(5,LONG2)
      CALL MOVEA(-106.91,1.00)
      CALL ANSTR(5,LONG3)
      CALL MOVEA(-106.81,1.00)
      CALL ANSTR(5,LONG4)
      CALL MOVEA(-106.78,0.00)
      CALL ANSTR(3,DEP1)
      CALL MOVEA(-106.78,-5.00)
      CALL ANSTR(3,DEP2)
      CALL MOVEA(-106.78,-10.00)
      CALL ANSTR(3,DEP3)
      CALL MOVEA(-106.78,-15.00)
      CALL ANSTR(3,DEP4)
      CALL ANNODE
      ACCEPT 514,B
514   FORMAT(F)
      CALL MOVEA(-106.95,0.00)
      CALL ANSTR(1,MARK)
      CALL MOVEA(-107.09,0.00)
      CALL ANSTR(1,MARK)
      CALL MOVEA(-106.96,0.00)
      CALL ANSTR(1,MARK)
      CALL MOVEA(-107.00,0.00)
      CALL ANSTR(1,MARK)
      CALL MOVEA(-106.99,0.00)
      K=K+1
      IF(K.GT.FLAG)GO TO 715
      GO TO 714
715   CALL ANNODE
      ACCEPT 555,C
555   FORMAT(F)
      STOP
      END
714   X=RAWT(K,2)
      Y=RAWT(K,3)
      CALL DRAWA(X,Y)
      CALL MOVEA(-106.95,0.00)
```

```
C
C PLOT THE LOCATIONS OF THE STATIONS USED IN THIS STUDY
C
      CALL MOVEA(-106.95,0.30)
      CALL ANSTR(2,NT)
      CALL MOVEA(-107.10,0.30)
      CALL ANSTR(2,SC)
      CALL MOVEA(-106.97,0.30)
      CALL ANSTR(2,CM)
      CALL MOVEA(-107.01,0.30)
      CALL ANSTR(2,IC)
      CALL MOVEA(-106.99,0.30)
      CALL ANSTR(2,WK)
      CALL MOVEA(-106.95,0.00)
      K=1
C
C FIND LOCATION OF ANOMOLOUS HYPOCENTERS AND DRAW RAYPATHS TO THEM
C FROM STATION COORDINATE
C
```

APPENDIX IV.

The cross-sectional and areal views of anomalous raypaths to the stations used in the study.

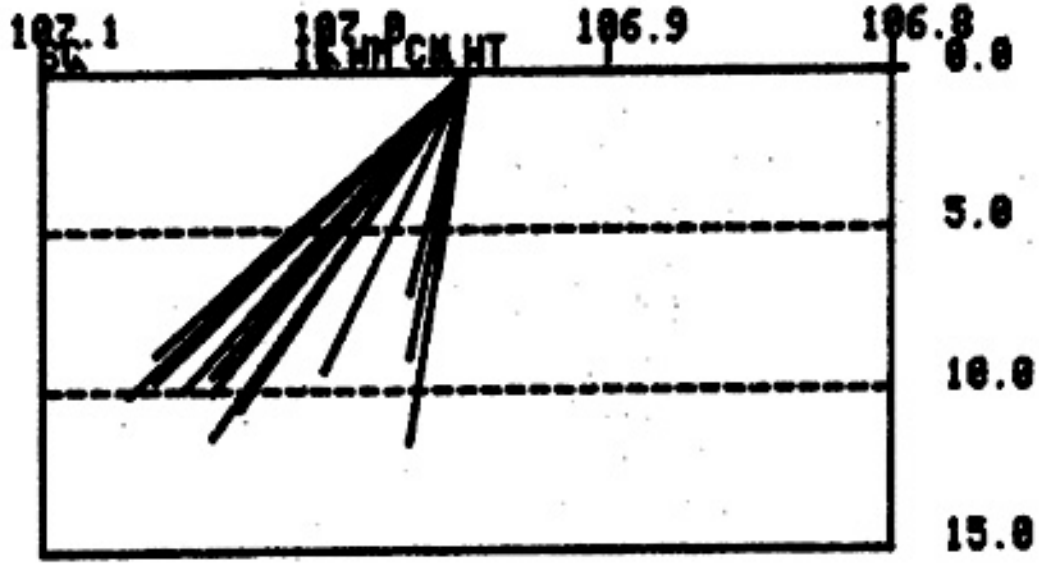
107.1
106.9
106.8
0.0
5.0
10.0
15.0

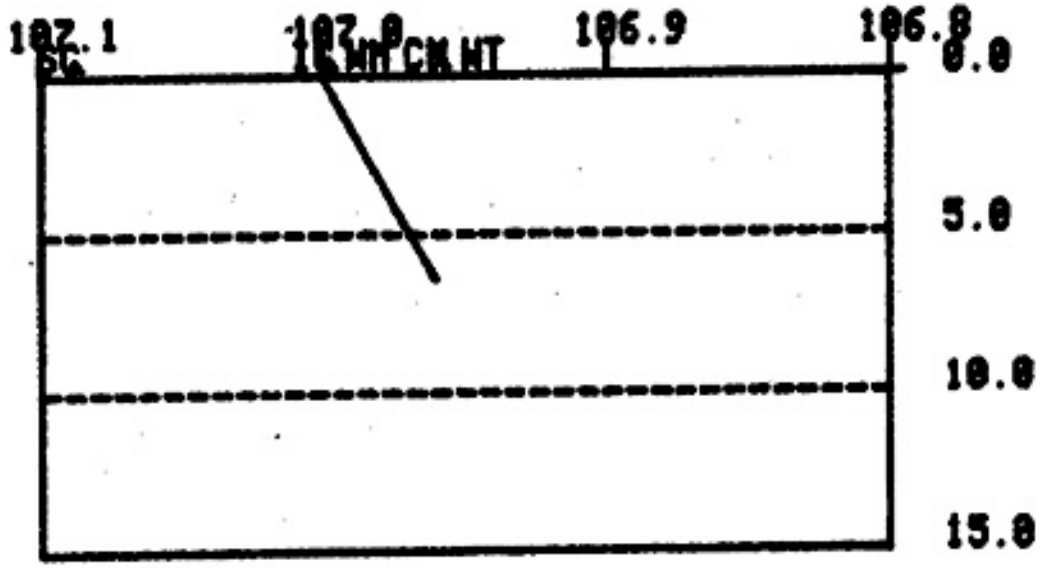
107.1
SC
107.0
MT CK MT
106.9
106.8
0.0
5.0
10.0
15.0

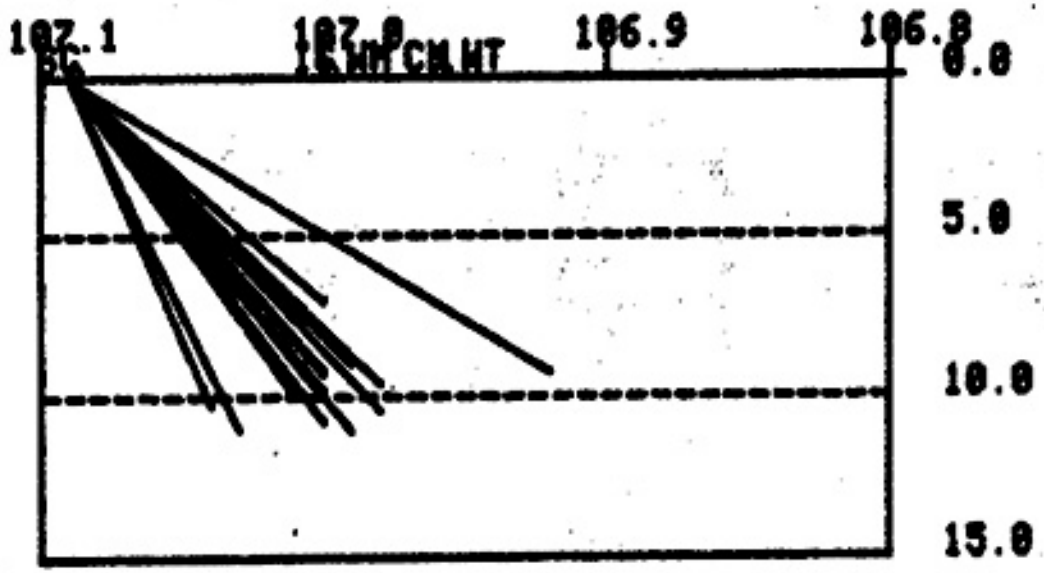
107.1
107.0
106.9
106.8
0.0
5.0
10.0
15.0

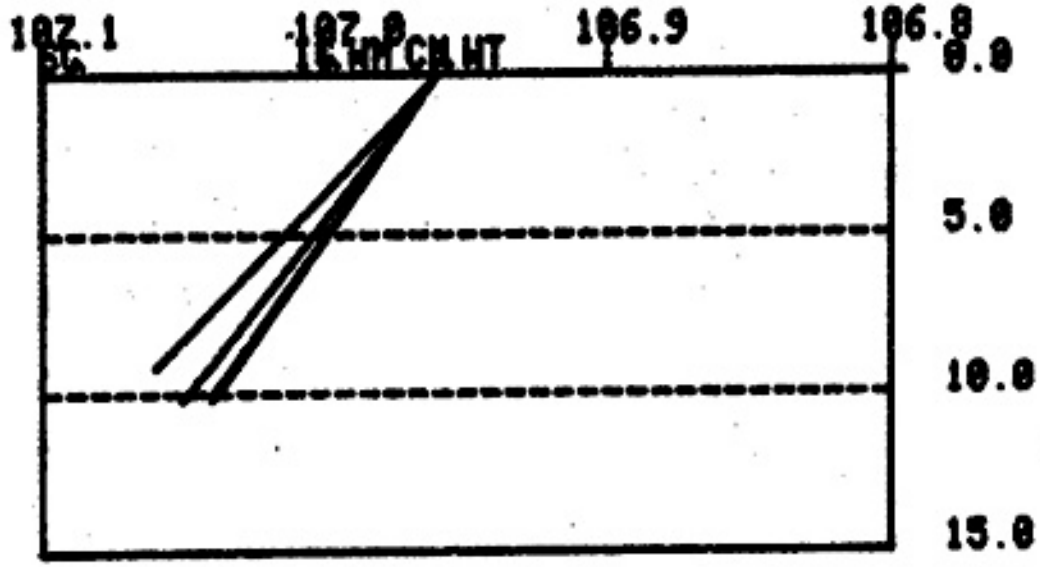
107.1
SC
107.0
15 MT CM HT
106.9
106.8
0.0
5.0
10.0
15.0

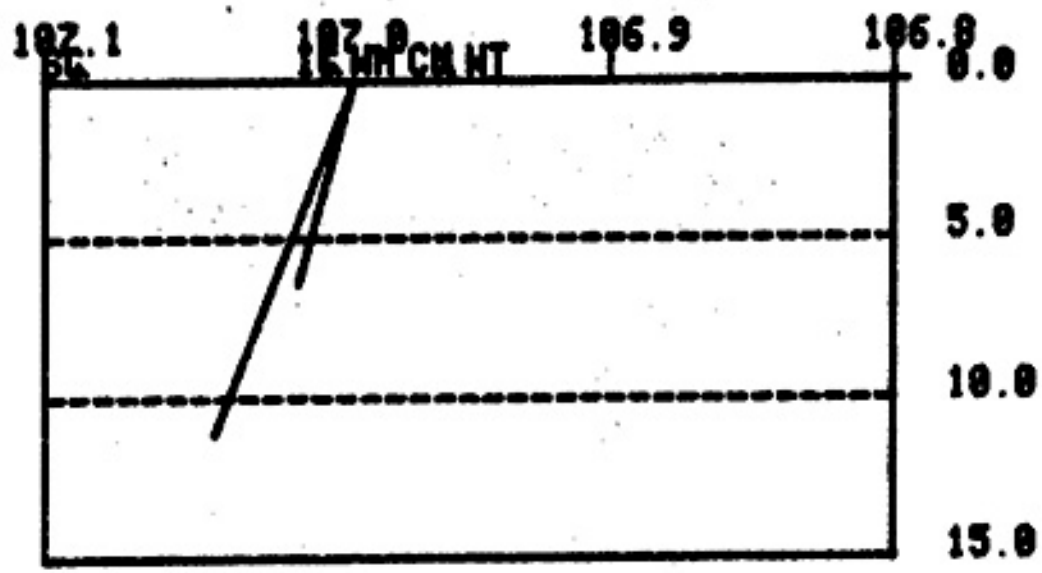
102.1
SL
107.0
16 MT CM MT
106.9
106.8
0.0
5.0
10.0
15.0

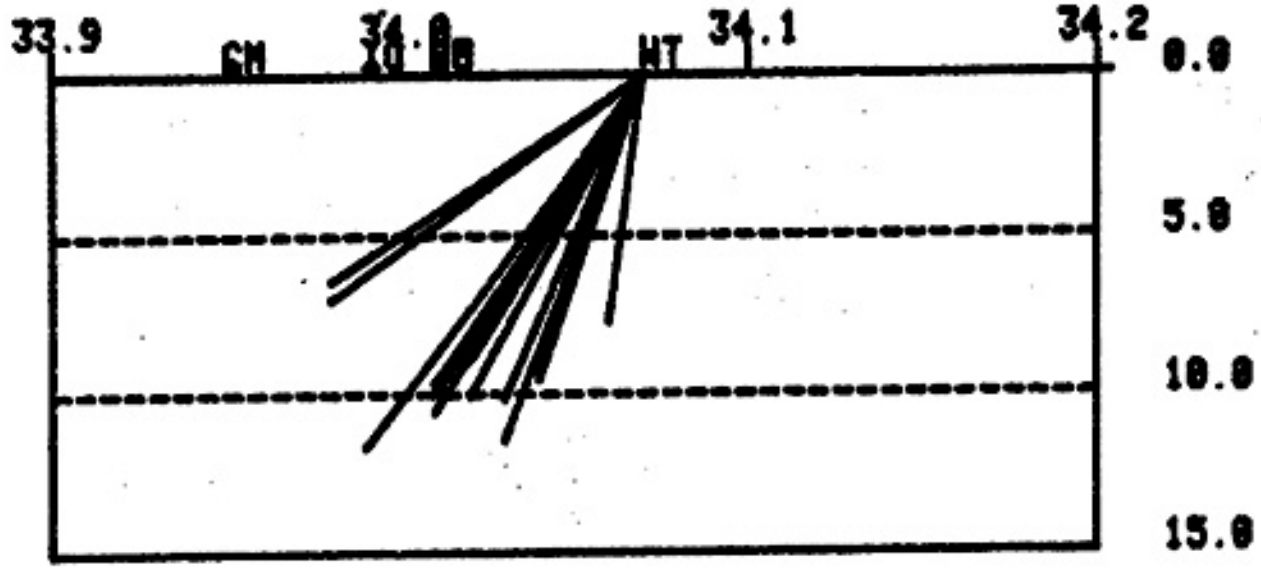
33.9
GM
34.0
34.1
34.2
0.0
5.0
10.0
15.0

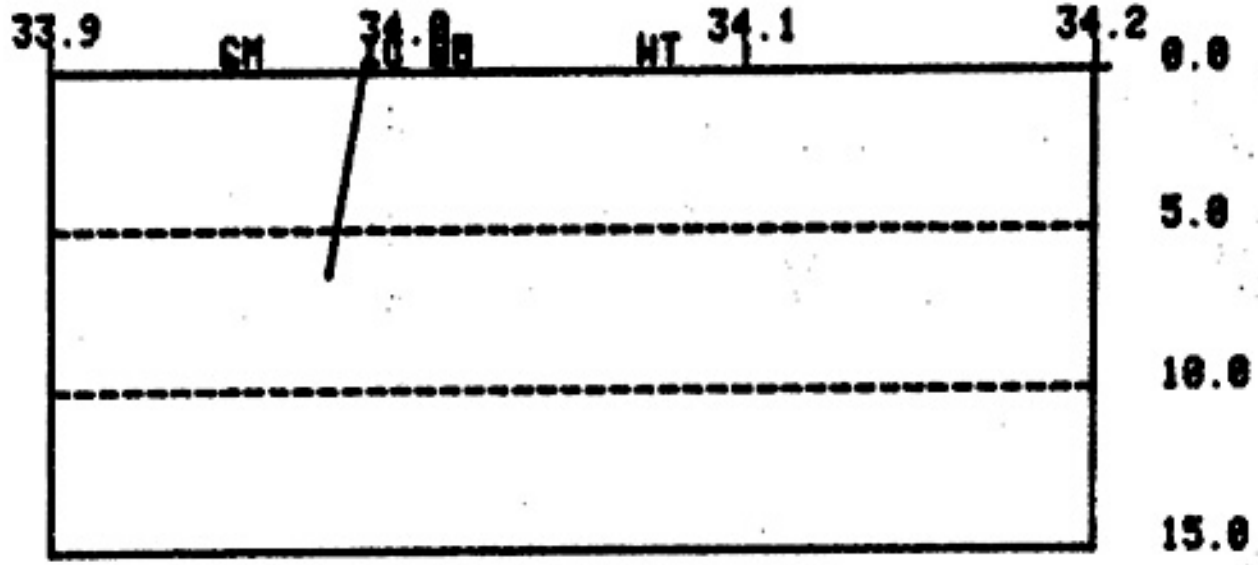
33.9
CM
34.0
MT
34.1
34.2
0.0
5.0
10.0
15.0

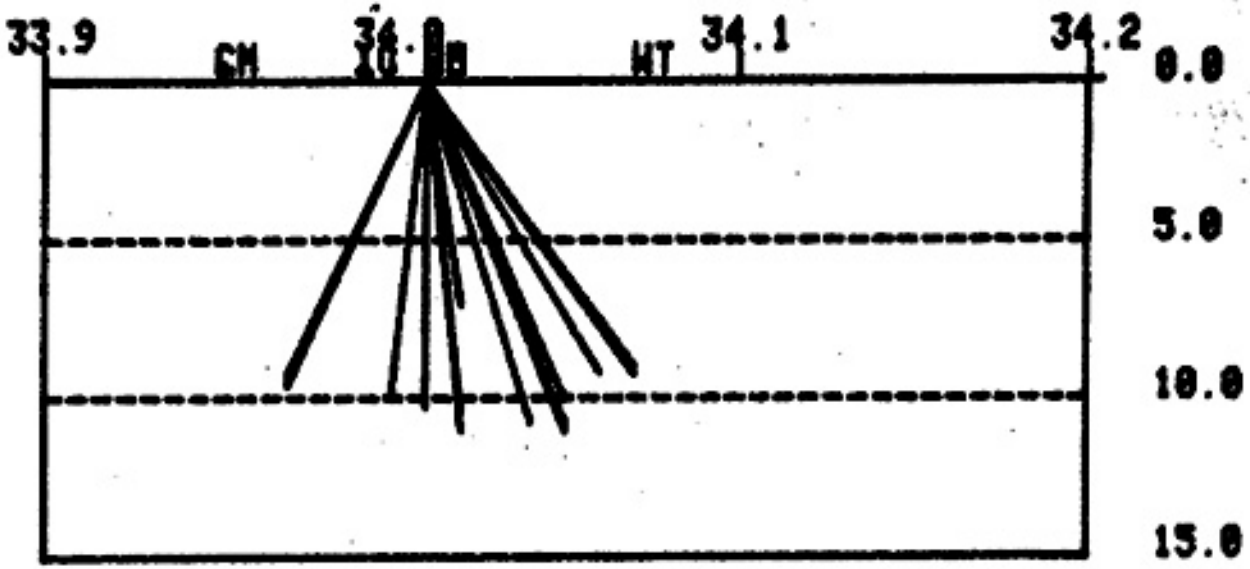
33.9
34.1
34.2
0.0
5.0
10.0
15.0

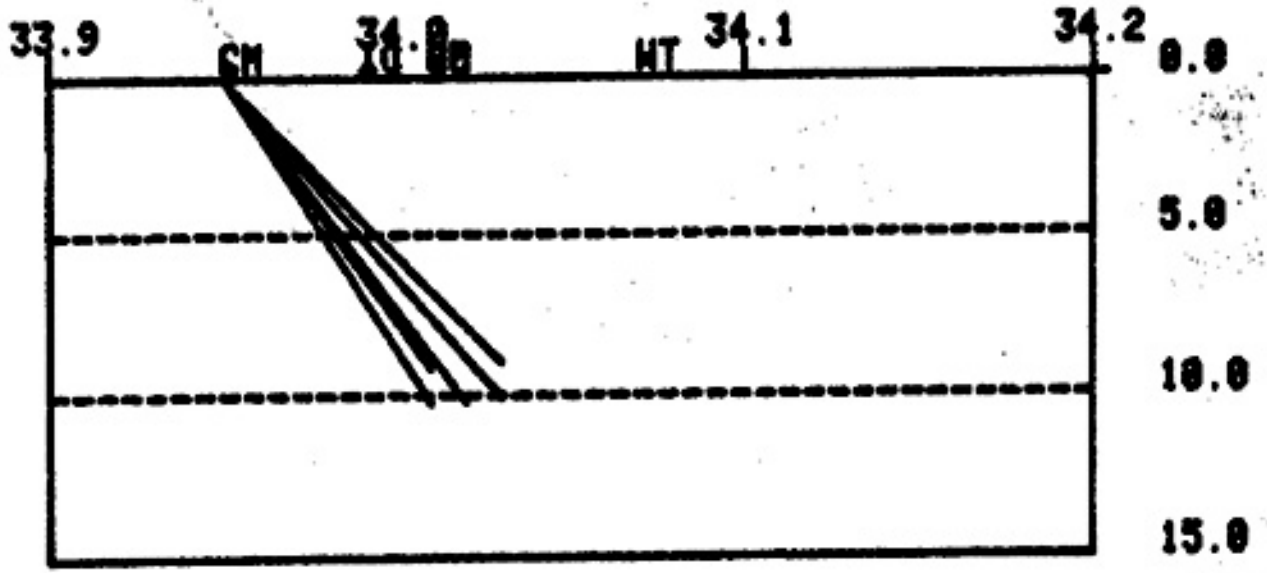
33.9
CM
34.0
34.1
HT
34.2
0.0
5.0
10.0
15.0

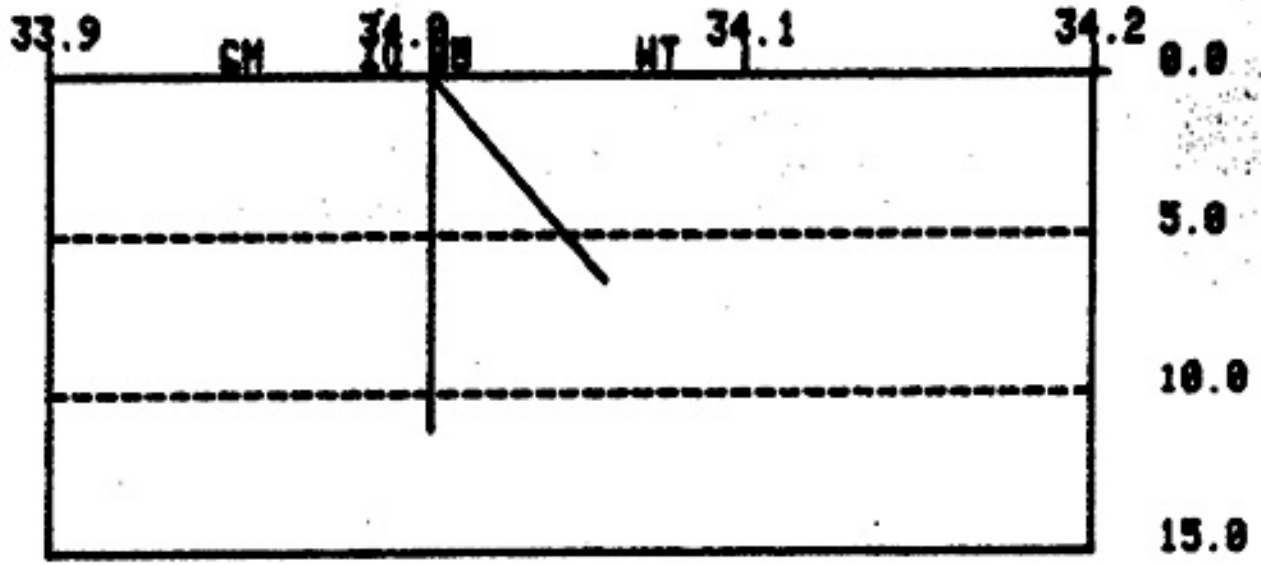
33.9
CM
34.1
HT
34.2
0.0
5.0
10.0
15.0

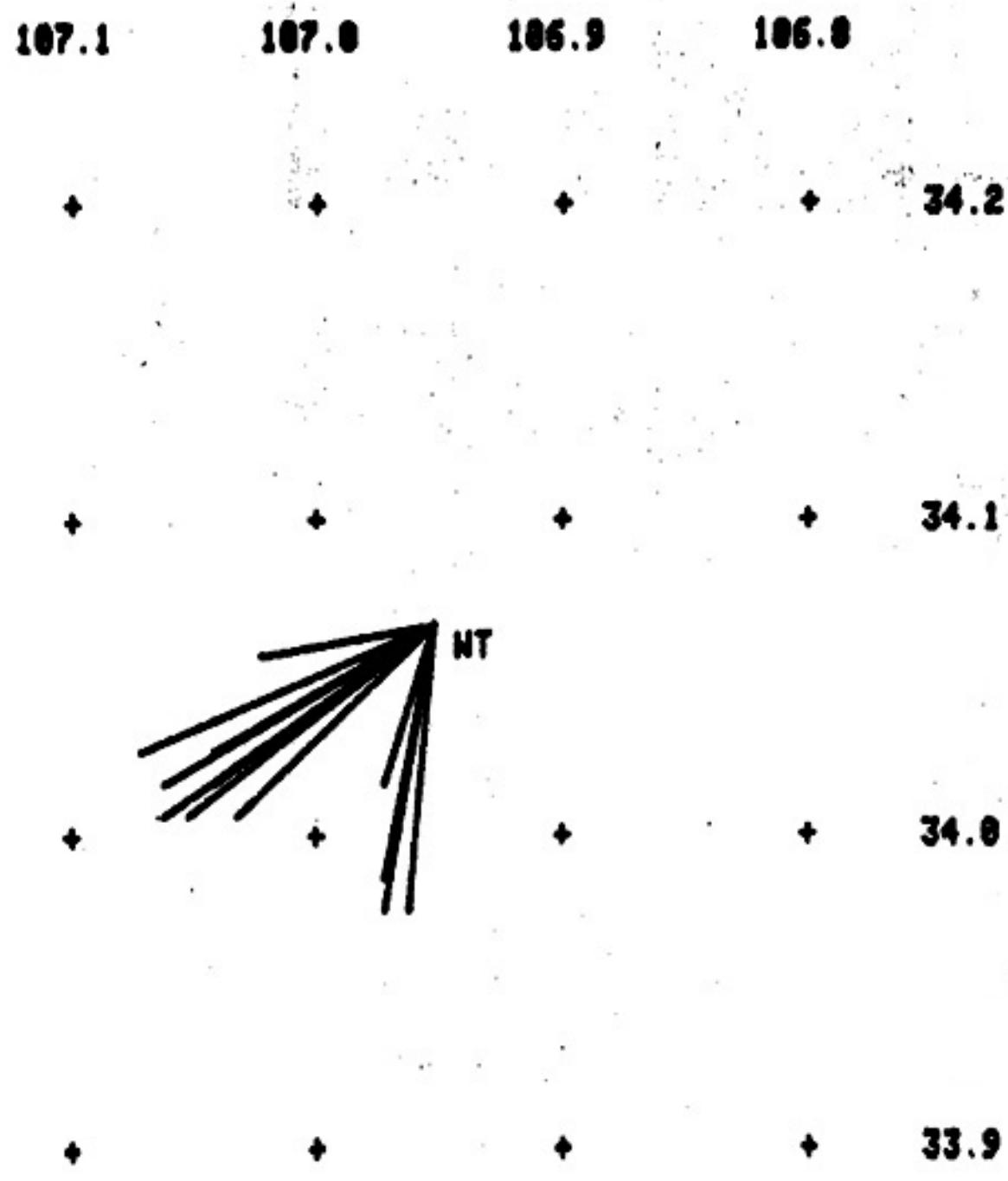
107.1
107.0
106.9
106.8
34.2
34.1
NT
34.0
33.9

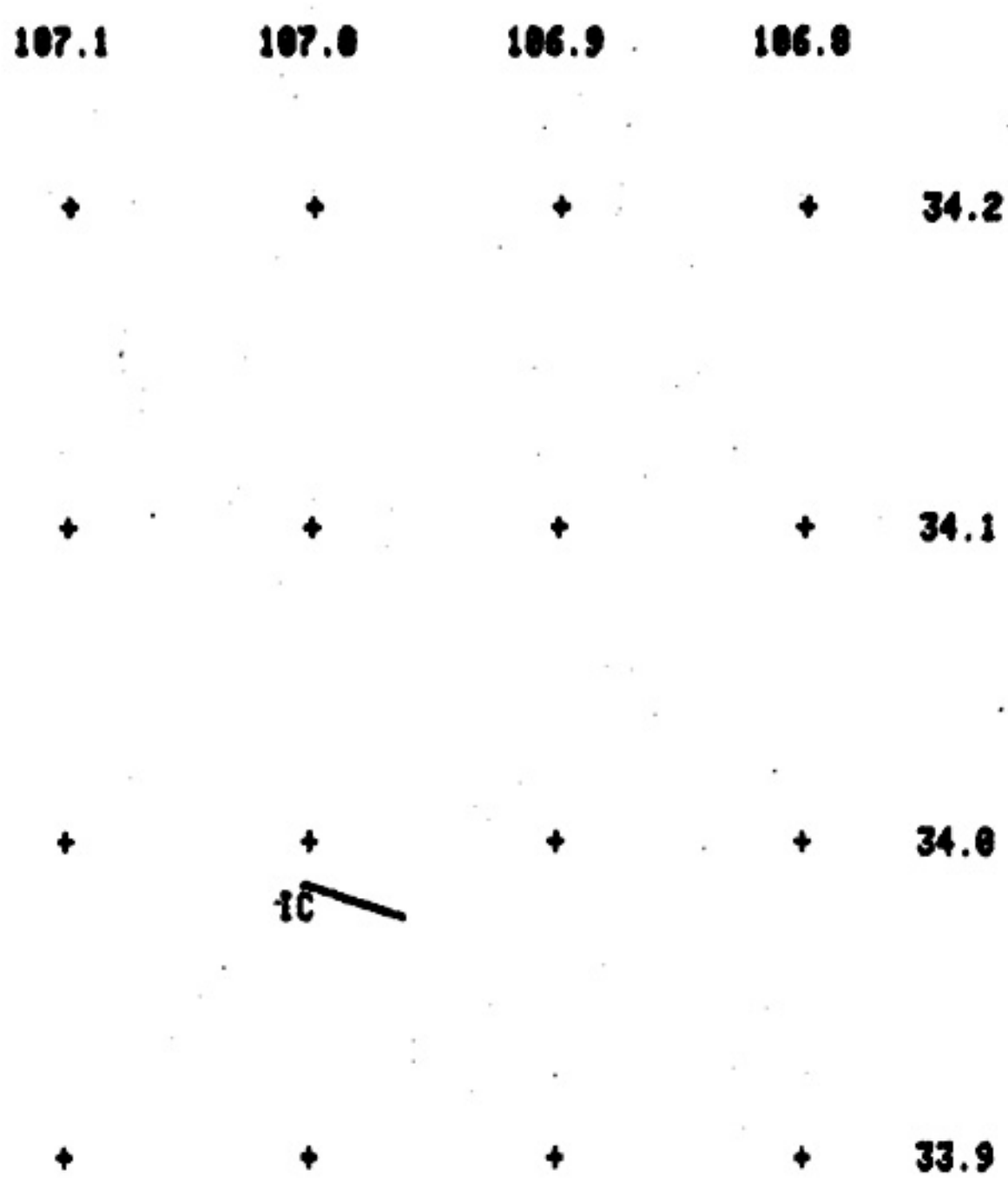
107.1
107.0
106.9
106.8
34.2
34.1
34.0
33.9

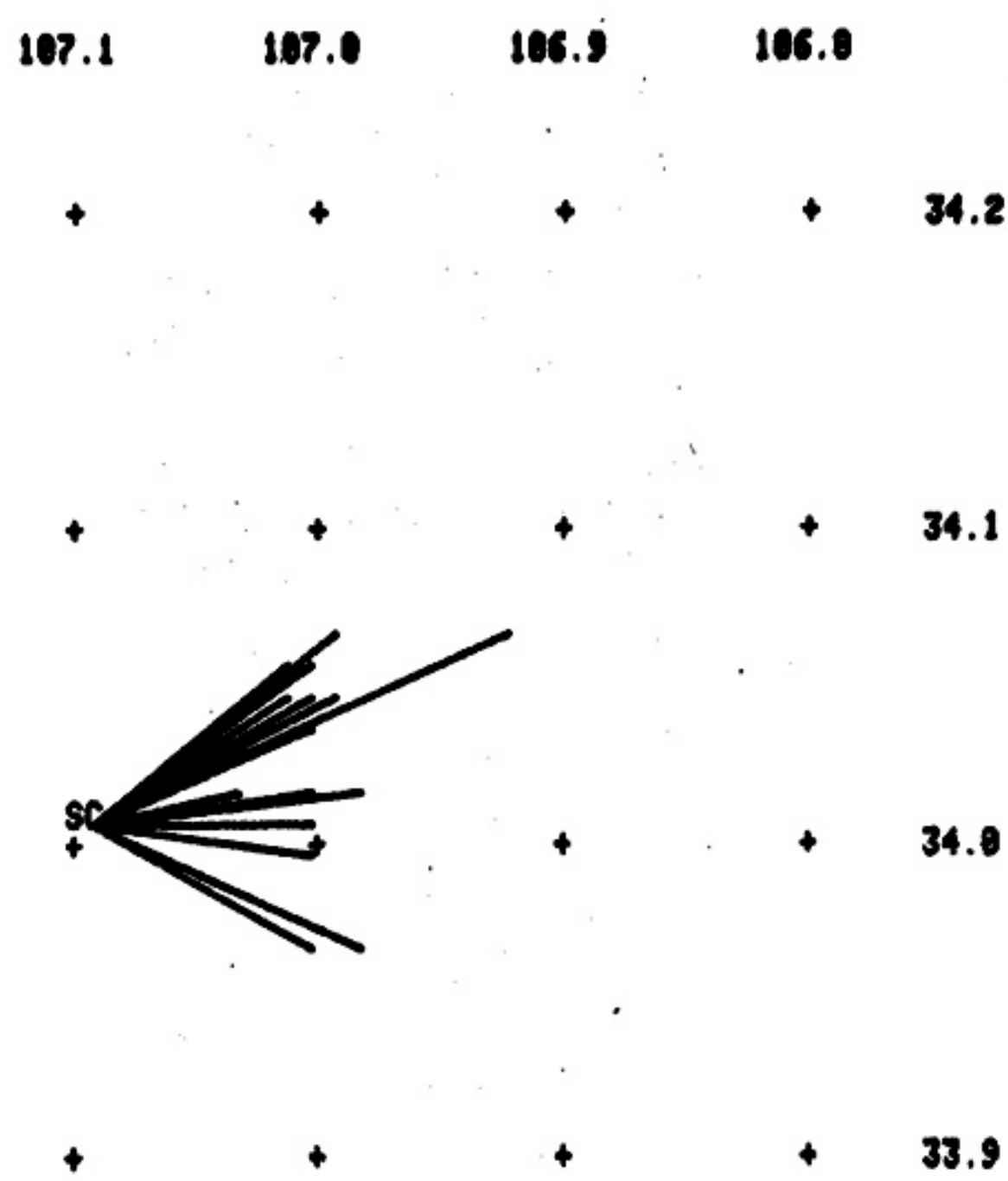
187.1
187.0
186.9
186.8
34.2
34.1
SC
34.0
33.9

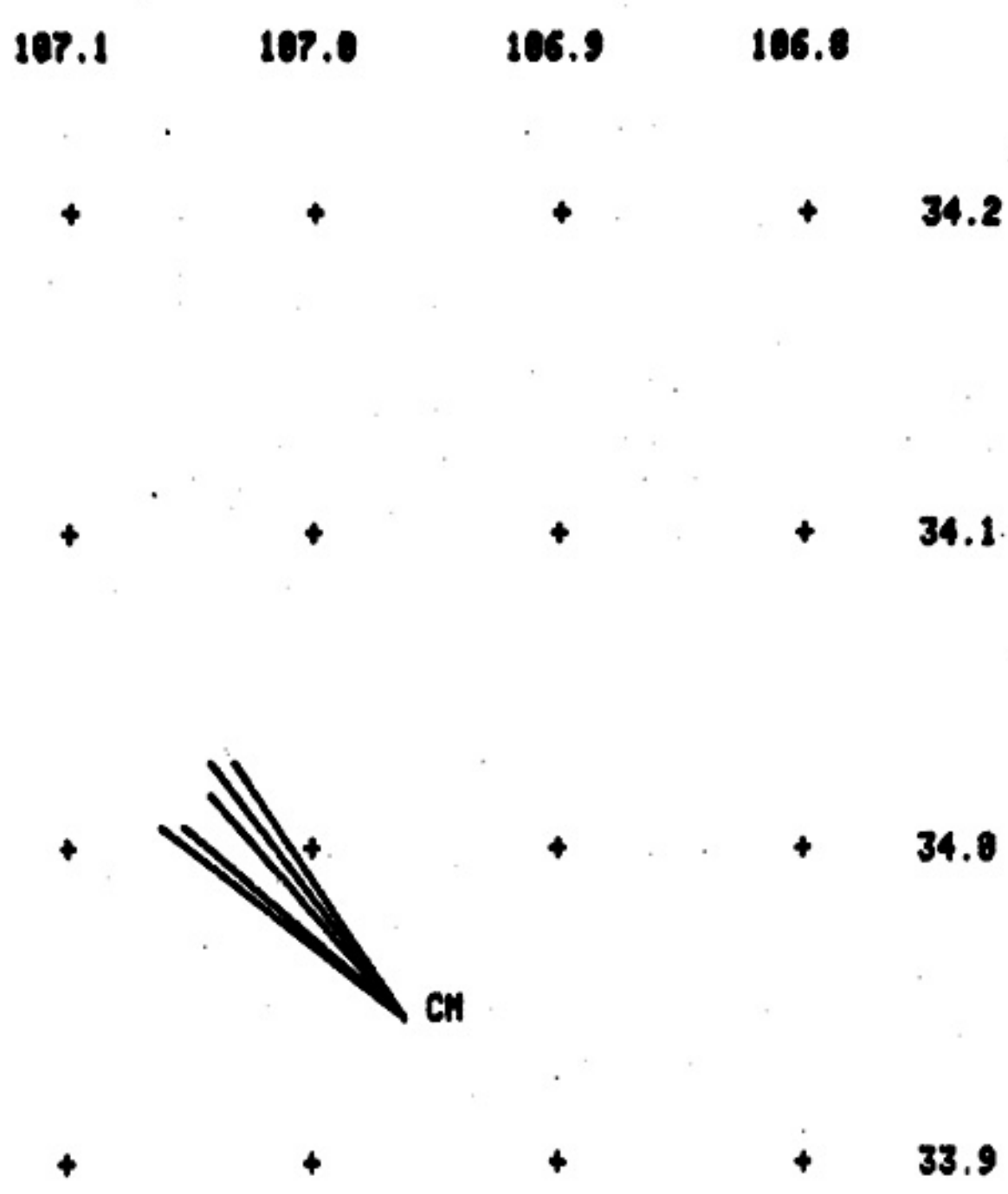

(74)

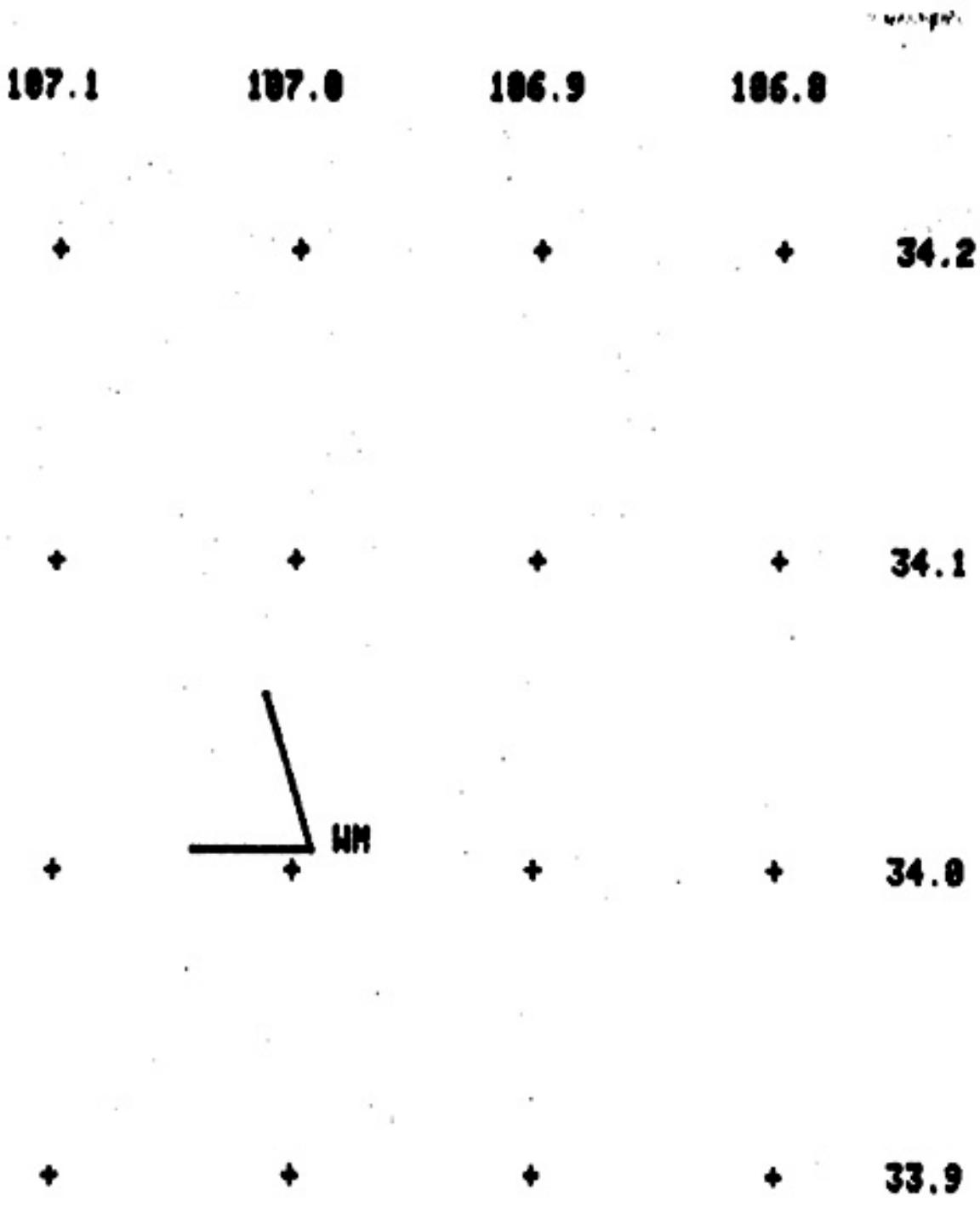

(52)

APPENDIX V.

The cross-sectional and areal views of non-anomalous raypaths to the stations used in the study.

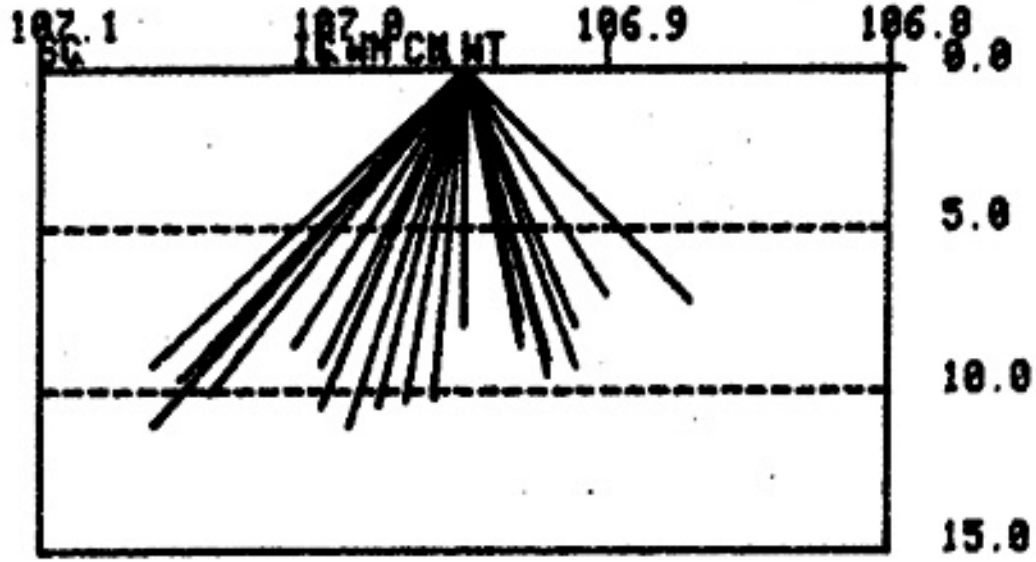
107.1
107.0
106.9
106.8
SC
KM
CK
MT
0.0
5.0
10.0
15.0

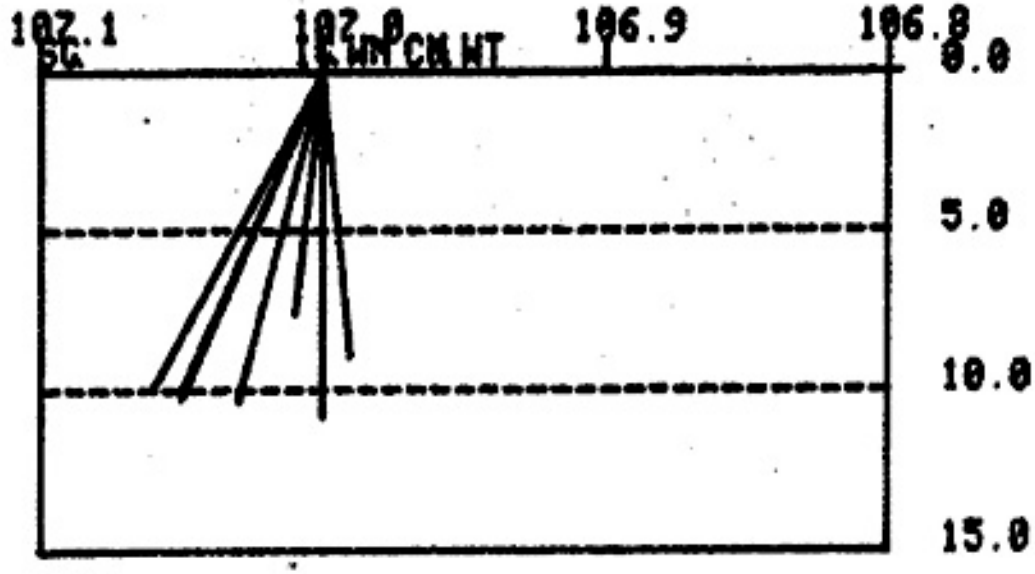
107.1
SG
107.0
106.9
106.8
0.0
5.0
10.0
15.0

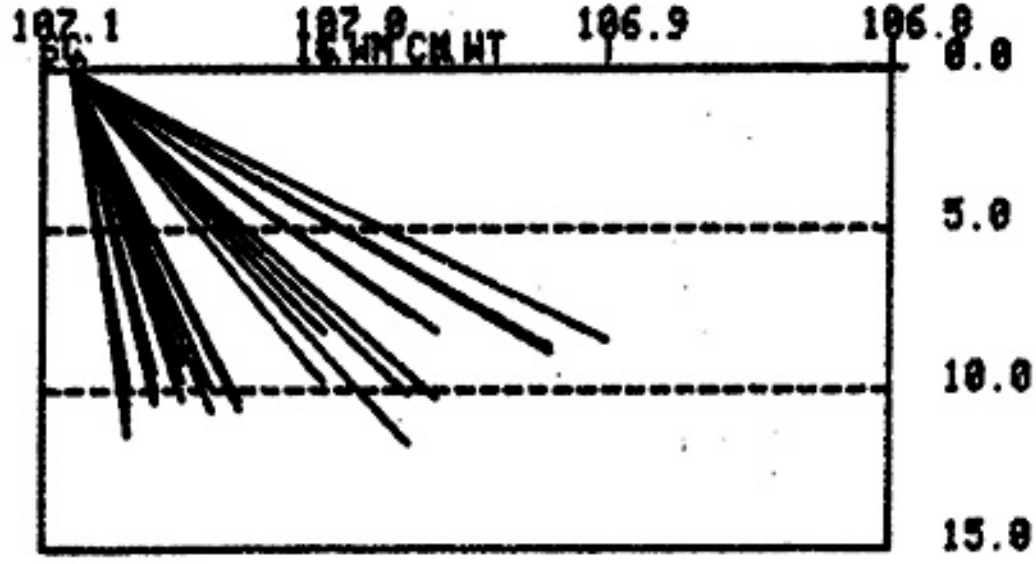
107.1
107.9
106.9
106.8
0.0
5.0
10.0
15.0

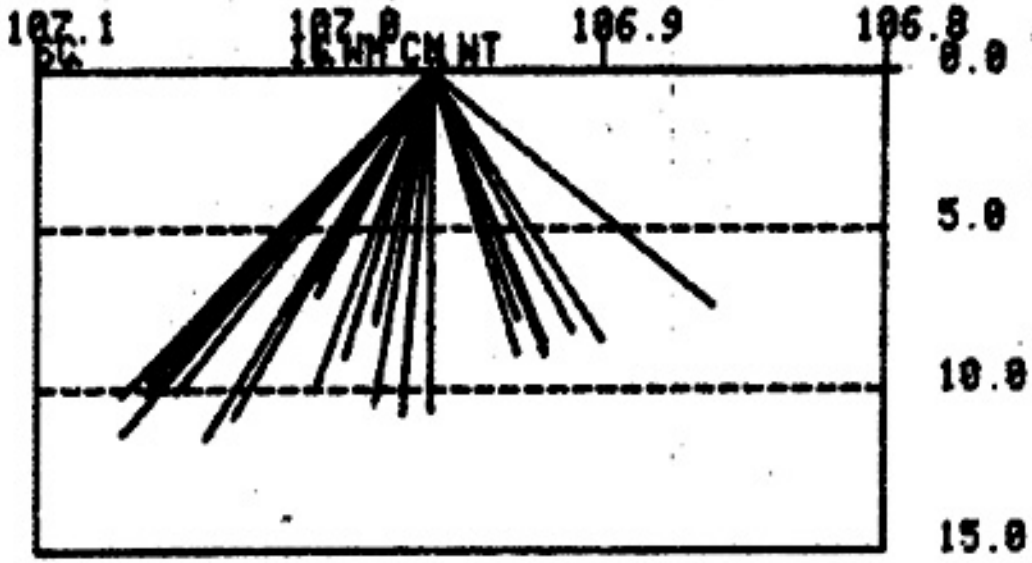
107.1
107.0
106.9
106.8
0.0
5.0
10.0
15.0

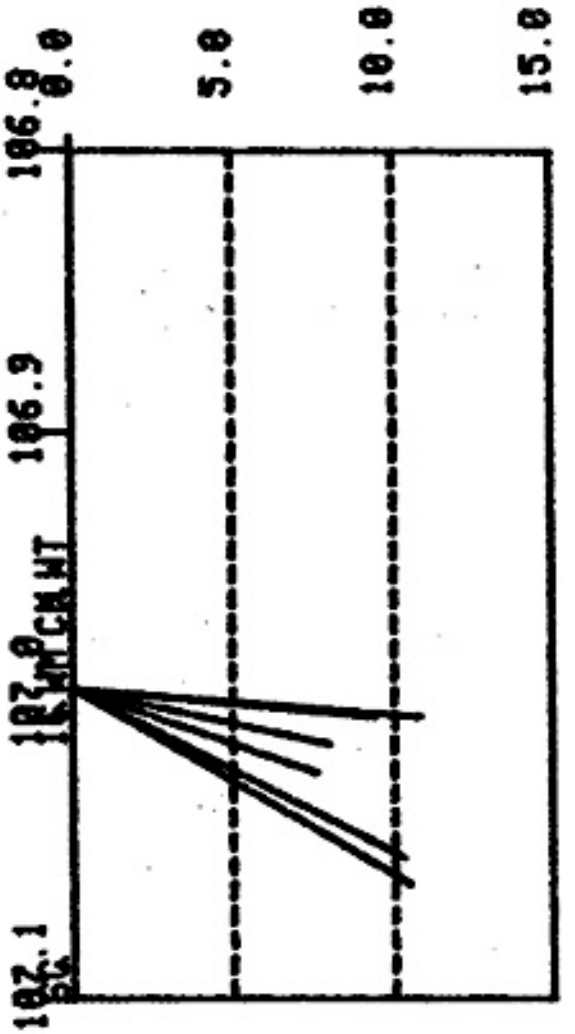
0.0
5.0
10.0
15.0
106.8
106.9
107.0
107.1
CM HT

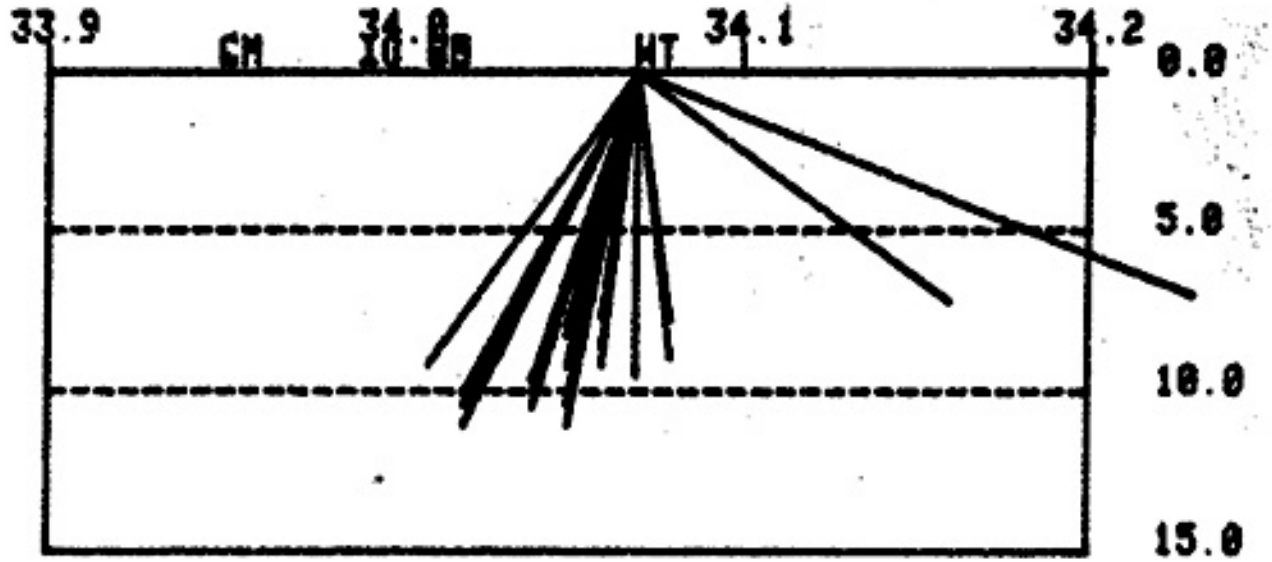
33.9
34.1
34.2
0.0
5.0
10.0
15.0

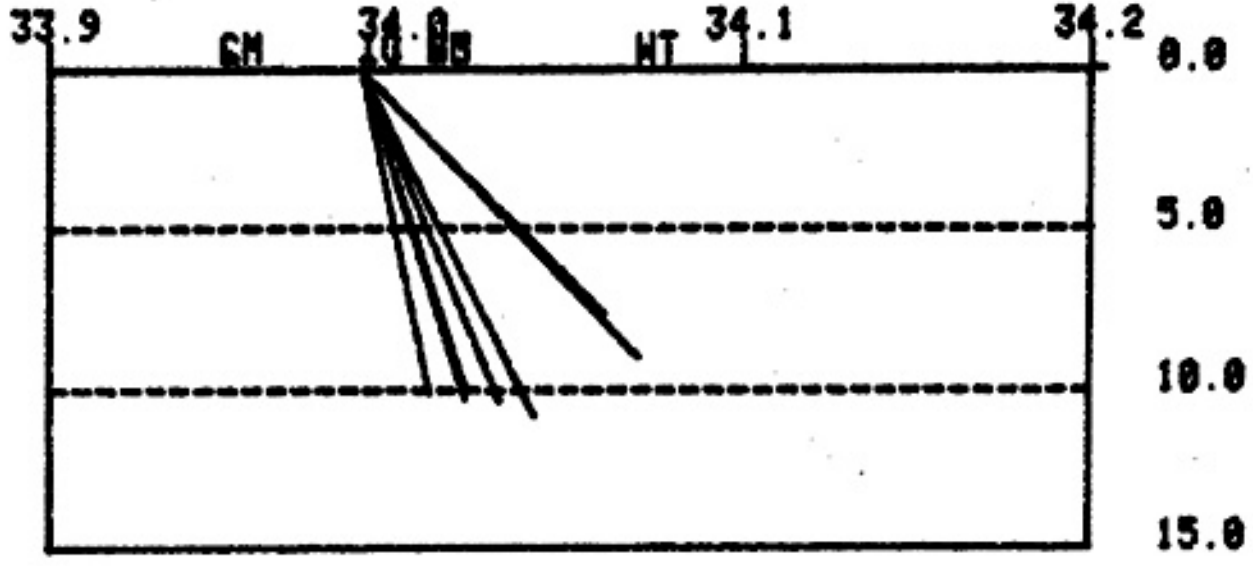
33.9
GM
34.0
HT
34.1
34.2
0.0
5.0
10.0
15.0

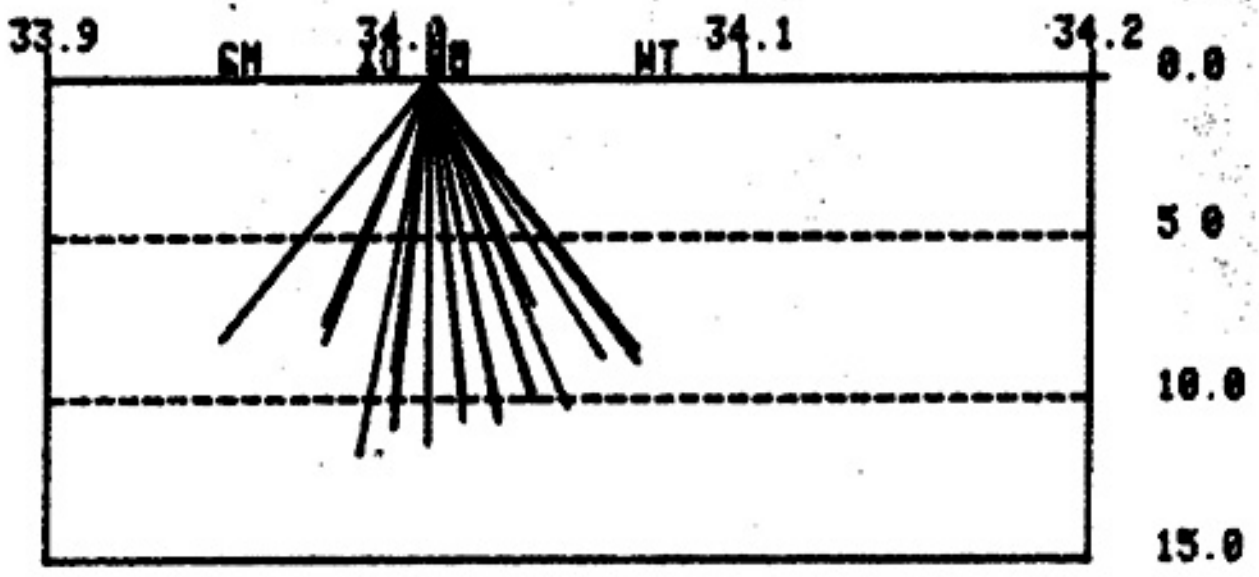
33.9
GM
34.0
MT
34.1
34.2
0.0
5.0
10.0
15.0

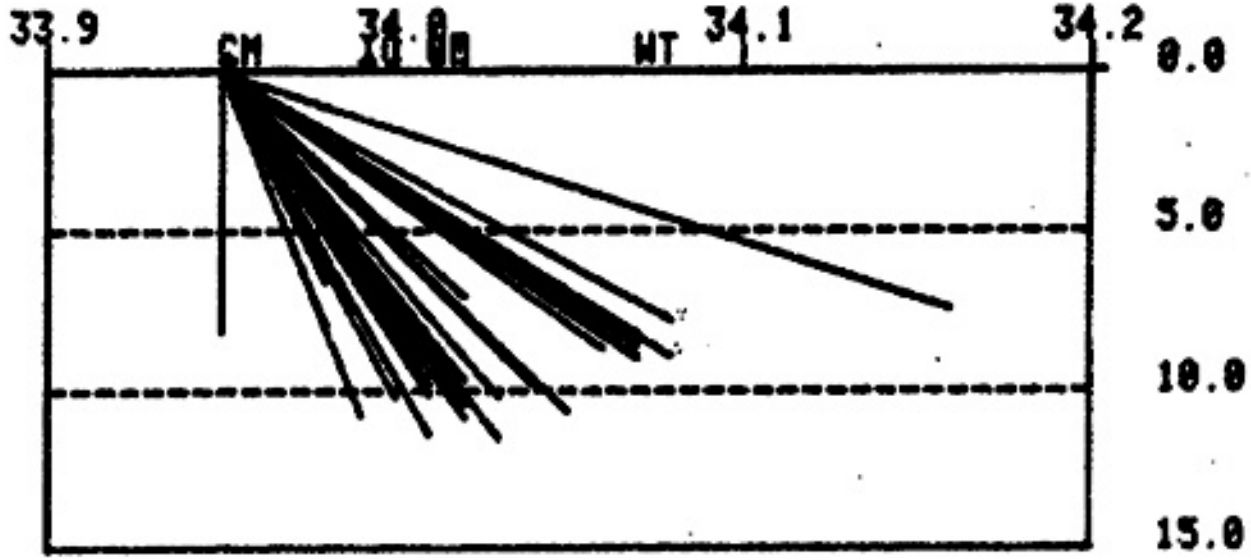
33.9
34.1
34.2
0.0
5.0
10.0
15.0

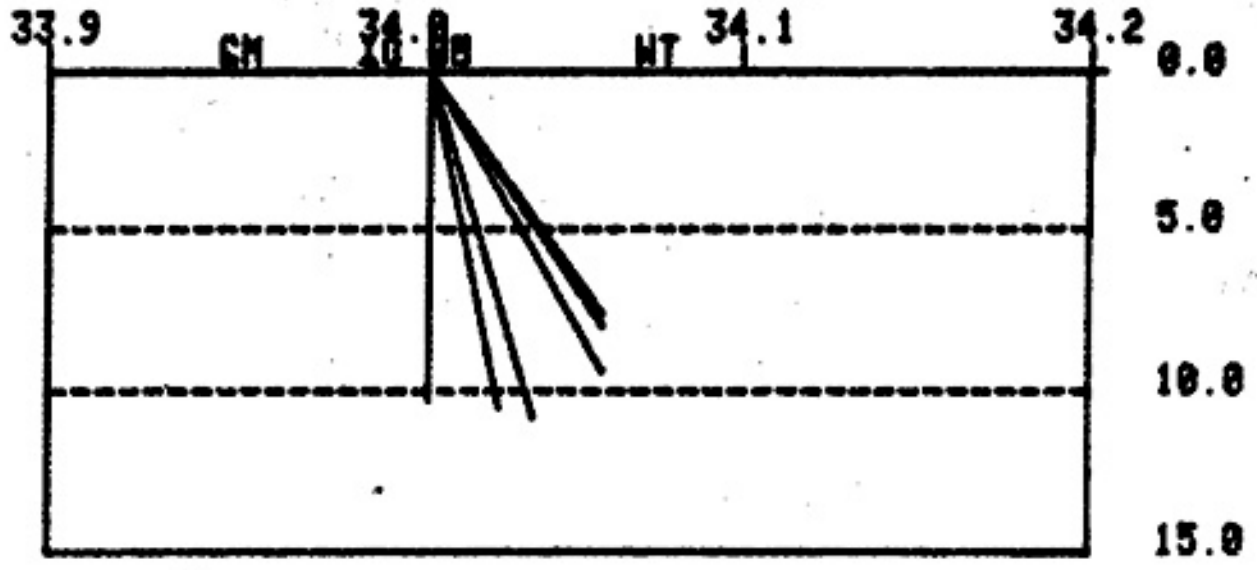
33.9
34.1
34.2
0.0
5.0
10.0
15.0

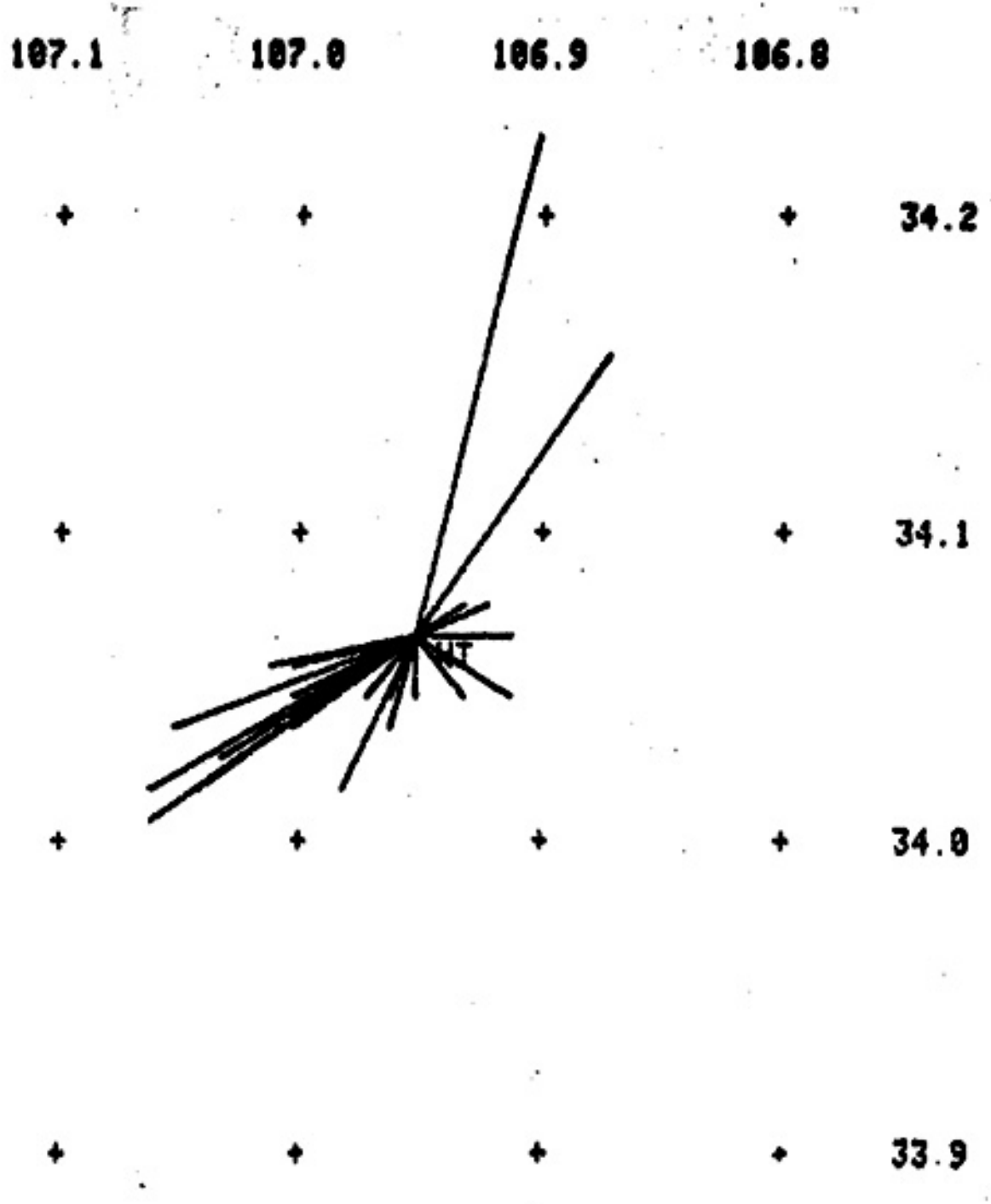
107.1
107.0
106.9
106.8
34.2
34.1
34.0
33.9

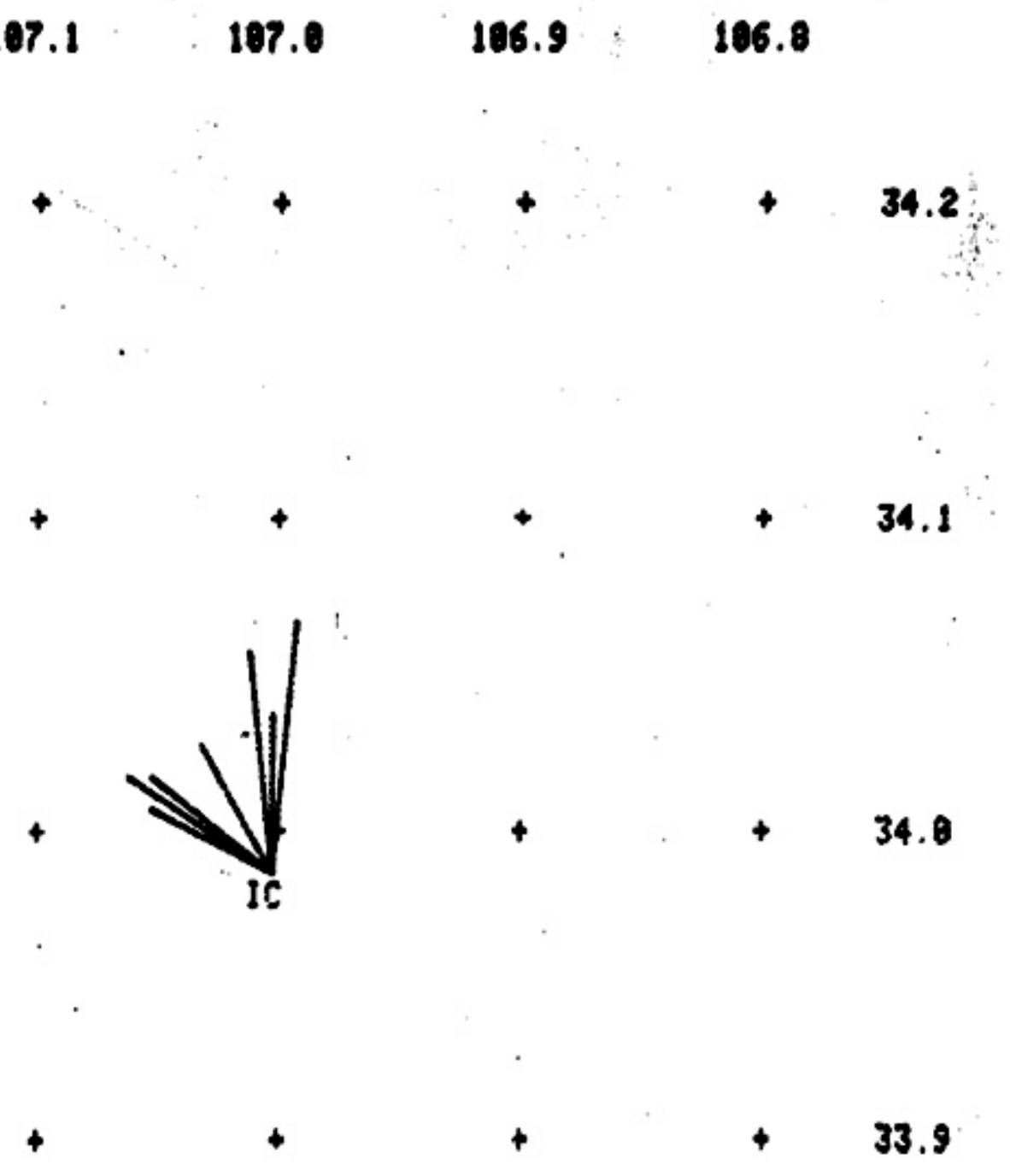
107.1
107.0
106.9
106.8
34.2
34.1
34.0
33.9
IC

107.1 107.0 106.9 106.8

34.2

34.1

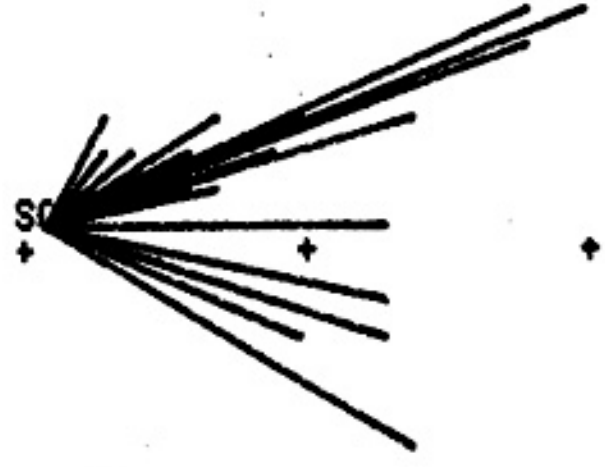

34.0

33.9

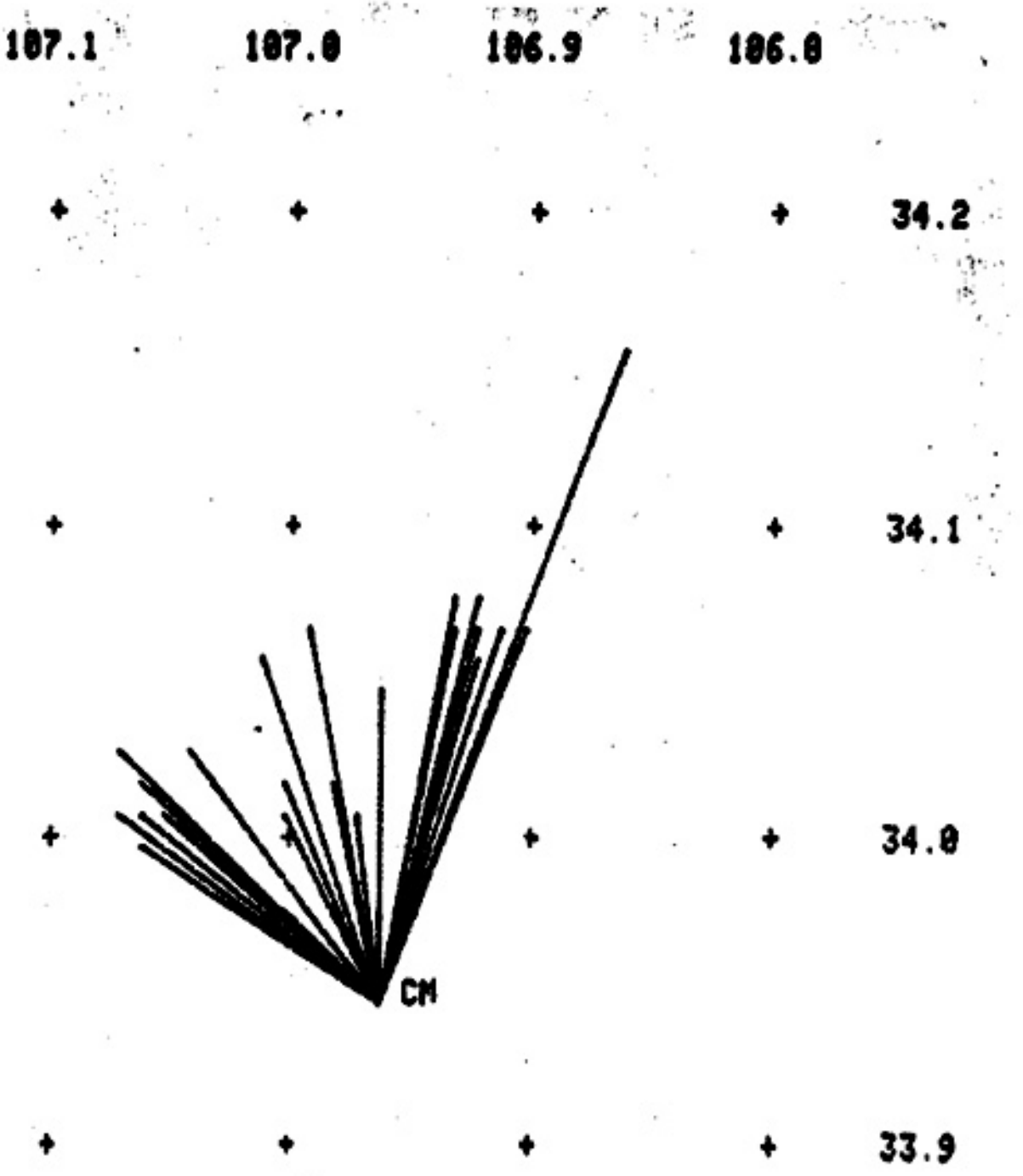

(06)

107.1 107.0 106.9 106.8

34.2

34.1

NM

34.0

33.9